



EDGEWOOD CHEMICAL BIOLOGICAL CENTER

U.S. ARMY RESEARCH, DEVELOPMENT AND ENGINEERING COMMAND
Aberdeen Proving Ground, MD 21010-5424

ECBC-TR-971

FINAL REPORT: STORAGE DEVICE/PACKAGE FOR TITANIUM DIOXIDE PARTICLES



Madhu Anand
Peter Hobbs

HALIDE GROUP, INC.
Bethlehem, PA 18015-2171

Al Kaziunas
Beth Campion

APPLIED SEPARATIONS, INC.
Allentown, PA 18101-1114

Brendan DeLacy

RESEARCH AND TECHNOLOGY DIRECTORATE

September 2012

Approved for public release; distribution is unlimited.



Disclaimer

The findings in this report are not to be construed as an official Department of the Army position unless so designated by other authorizing documents.

REPORT DOCUMENTATION PAGE				Form Approved OMB No. 0704-0188	
Public reporting burden for this collection of information is estimated to average 1 hour per response, including the time for reviewing instructions, searching existing data sources, gathering and maintaining the data needed, and completing and reviewing this collection of information. Send comments regarding this burden estimate or any other aspect of this collection of information, including suggestions for reducing this burden to Department of Defense, Washington Headquarters Services, Directorate for Information Operations and Reports (0704-0188), 1215 Jefferson Davis Highway, Suite 1204, Arlington, VA 22202-4302. Respondents should be aware that notwithstanding any other provision of law, no person shall be subject to any penalty for failing to comply with a collection of information if it does not display a currently valid OMB control number. PLEASE DO NOT RETURN YOUR FORM TO THE ABOVE ADDRESS.					
1. REPORT DATE (DD-MM-YYYY) XX-09-2012		2. REPORT TYPE Final		3. DATES COVERED (From - To) Jun 2010 - Sep 2011	
4. TITLE AND SUBTITLE Final Report: Storage Device/Package for Titanium Dioxide Particles				5a. CONTRACT NUMBER DAAD13-03-D-0014 - Task 64	
				5b. GRANT NUMBER	
				5c. PROGRAM ELEMENT NUMBER	
6. AUTHOR(S) Anand, Madhu; Hobbs, Peter (Halide Group, Inc.); Kaziunas, Al; Campion, Beth (Applied Separations); and DeLacy, Brendan (ECBC)				5d. PROJECT NUMBER	
				5e. TASK NUMBER	
				5f. WORK UNIT NUMBER	
7. PERFORMING ORGANIZATION NAME(S) AND ADDRESS(ES) Halide Group, Inc., 205 Webster Street, Bethlehem, PA 18015-2171 Applied Separations, Inc., 930 Hamilton Street, Allentown, PA 18101-1114 Director, ECBC, ATTN: RDCB-DRT-S, APG, MD 21010-5424				8. PERFORMING ORGANIZATION REPORT NUMBER ECBC-TR-971	
9. SPONSORING / MONITORING AGENCY NAME(S) AND ADDRESS(ES)				10. SPONSOR/MONITOR'S ACRONYM(S)	
				11. SPONSOR/MONITOR'S REPORT NUMBER(S)	
12. DISTRIBUTION / AVAILABILITY STATEMENT Approved for public release; distribution is unlimited.					
13. SUPPLEMENTARY NOTES					
14. ABSTRACT The overall goal of this project was to generate information to help improve the performance of titanium dioxide (TiO ₂) dispersal grenades used for visual obscuration. The study evaluated ways to improve the performance of TiO ₂ through the investigation of the impact of adsorbed water on the TiO ₂ obscuration performance and techniques for moisture removal, along with the evaluation of handling and packaging to maintain the "dry" state. Improvement would be manifested by increased obscurance and/or longer obscuration times for the same size grenade and the same volume and/or weight load of obscurant particles.					
15. SUBJECT TERMS Titanium dioxide Visible obscurant Coatings Particle size Characterization					
16. SECURITY CLASSIFICATION OF:			17. LIMITATION OF ABSTRACT UU	18. NUMBER OF PAGES 68	19a. NAME OF RESPONSIBLE PERSON Renu B. Rastogi
a. REPORT U	b. ABSTRACT U	c. THIS PAGE U			19b. TELEPHONE NUMBER (include area code) (410) 436-7545

Blank

EXECUTIVE SUMMARY

The obscurance obtained from “smoke” grenades that are based on current TiO_2 particulate loadings in the devices falls far below the theoretical performance that should be obtained when the mass loadings of TiO_2 are provided. As part of the U.S. Army’s efforts to improve its overall defeat technologies, this work investigated some of the potential factors that may have limited the dispersal performance of the TiO_2 powders.

The use of supercritical carbon dioxide (SCCO_2), a fluid with zero surface tension, was investigated for the removal of trace moisture and/or solvents from the surface of the TiO_2 obscurant powders. The lack of surface tension means an absence of capillary forces, which normally cause particle agglomeration on drying.

The role of sorbed moisture on the settling time for TiO_2 obscurant powders was investigated using the currently employed hydrophobic TiO_2 as well as five other forms—one alternative commercial and three custom-modified hydrophobic TiO_2 forms and an unmodified hydrophilic TiO_2 . When the drying was performed in SCCO_2 , the laboratory-measured settling time for all of the sampled materials increased after drying. To a lesser extent, thermal drying also increased the settling time for most of the tested powders.

Hydrophilic TiO_2 particles were also coated with organosilanes and fluorosilanes, using SCCO_2 as the solvent for the silanes. These powders were comparable to the commercially coated and Army-coated (both coated with organosilanes) TiO_2 powders in laboratory aerosolization and moisture analysis tests.

The increased settling time after SCCO_2 drying or coating with silanes from SCCO_2 did not translate into an improved TiO_2 performance during the larger scale testing in the U.S. Army’s 190 m^3 test facility using the Stanford Reference Institute (SRI) nozzle or explosive dissemination. Testing the kinetics of moisture uptake on all of the dried powders showed moisture uptake approaching equilibrium with the ambient humidity levels. The uptake with the ambient humidity levels was very rapid, at <10 min for small samples to approach equilibrium.

Packaging tests using commercial “off-the-shelf” metalized polymer bags demonstrated that dried and properly packaged TiO_2 powders retained their improved settling times for extended periods of >2 months, which was the duration of the rest of the time in this study.

During characterization of the sample powders, it was found that relatively moderate shear forces were sufficient to deagglomerate all of the powders to a particle diameter of approximately twice that of the fundamental particle size of the powders.

The overall goal of this project was to generate information to help improve the performance of TiO_2 dispersal grenades used for visual obscuration. The study evaluated ways to improve the performance of TiO_2 through the investigation of the impact of adsorbed water on the TiO_2 obscuration performance techniques for moisture removal, along with the evaluation of

handling and packaging to maintain the “dry” state. Improvement would be manifested by increased obscurance and/or longer obscuration times for the same size grenade and the same volume and/or weight load of obscurant particles.

The major objective was to improve the dispersion of the current particles used in the grenade and/or to identify a potential replacement or modified TiO_2 particle for use in these grenades so that the particles aerosolize more efficiently and remain aerosolized longer after detonation.

PREFACE

The work described in this report was authorized under contract no. DAAD13-03-D-0014, Task 64 with SciTech Services (Havre de Grace, MD). This work was started in January 2010 and completed in September 2011.

The use of either trade or manufacturers' names in this report does not constitute an official endorsement of any commercial products. This report may not be cited for purposes of advertisement.

This report has been approved for public release. Registered users should request additional copies from the Defense Technical Information Center; unregistered users should direct such requests to the National Technical Information Service.

Acknowledgments

The authors wish to thank James Shomo of the U.S. Army Edgewood Chemical Biological Center (Aberdeen Proving Ground, MD) and Dennis Metz of SciTech Services (Havre de Grace, MD) for managing the contractual portion of this effort. The authors also wish to thank Randy Loiland and Nolan Shaver of the Joint Program Manager (JPM) Nuclear, Biological, Chemical – Contamination Avoidance (NBC-CA) for their sponsorship of this effort. The authors would like to acknowledge Christine Franklin of Science Applications International Corporation (Gunpowder, MD) for administrative support.

Blank

CONTENTS

1.	INTRODUCTION	1
1.1	Background and Objectives	1
1.1.1	Visible Obscuration with TiO ₂ Particles	1
1.1.2	Figure of Merit	1
1.1.3	Materials Investigated and Base Performance	3
1.2	Project Tasks	5
2.	SET UP LABORATORY FOM CHARACTERIZATION TOOLS	6
2.1	Aerosolization Testers	6
2.2	Karl Fischer Moisture Analysis	9
2.3	Particle Shear Strength: Unconfined Yield Strength	10
2.4	Particle Size Characterization with Light Diffraction	11
2.5	Adaption of Applied Separations SCCO ₂ Equipment	12
3.	DRYING OF TiO ₂ PARTICLES WITH SCCO ₂ AND BY THERMAL TREATMENT	12
3.1	Thermal Drying of TiO ₂	13
3.2	SCCO ₂ Drying of TiO ₂	13
3.2.1	Scale-Up of SCCO ₂ Drying of TiO ₂	15
3.2.2	SCCO ₂ Drying of TiO ₂ with Agitation	20
4.	DEVELOP AND TEST PACKAGING FOR TiO ₂ PARTICLES	21
4.1	Baseline Data on Water Vapor Adsorption	21
4.2	Moisture Adsorption Kinetics	23
4.3	Packaging for Storage of TiO ₂ Particles	25
5.	COATING TiO ₂ PARTICLES FROM SCCO ₂	27
5.1	DPDMS Coating and Drying of Particles in SCCO ₂	27
5.2	Coating and Drying of Particles in SCCO ₂ with Agitation	28
6.	ECBC TESTING OF TiO ₂ POWDERS IN 190 m ³ TEST CHAMBER	29
6.1	Dissemination by SIR Nozzle	30
6.2	Dissemination by Explosives	32
6.3	Testing Fumed TiO ₂	33
7.	FUMED TiO ₂ : SMALLER PARTICLES FOR OBSCURATION	33

8.	HIGH SHEAR FOR PARTICLE DEAGGLOMERATION	33
9.	SUMMARY AND CONCLUSIONS	34
10.	IDEAS FOR FUTURE WORK	34
	LITERATURE CITED	37
	ACRONYMS AND ABBREVIATIONS	39
	APPENDICES:	
	A: UNCONFINED YIELD STRENGTH OF POWDERS	41
	B: HIGH SHEAR FOR PARTICLE DEAGGLOMERATION	45
	C: SMALLER PARTICLES FOR OBSCURATION	
	SUCH AS FUMED TiO ₂	51

FIGURES

1.	Laboratory FoM aerosolization tester	6
2.	Calculated settling times for TiO ₂ particles as a function of particle diameter, where the desired particle size is 0.25 μm	7
3.	Moisture analyzer set up in the lab	9
4.	MECs measured from the 190 m ³ chamber with the use of the SRI nozzle	17
5.	Particle size and yield of small particles in NanoComposix obscuration chamber	18
6.	Particle size and yield of large particles in NanoComposix obscuration chamber	19
7.	Effect of moisture content on settling time in aerosolization chamber	22
8.	Moisture uptake rate: RCL-9	23
9.	Moisture uptake rate: RCL-9/DPDMS	23
10.	Moisture uptake rate: Tiona 188	24
11.	Moisture uptake rate: CR 470	24
12.	Settling time vs moisture content for coating DPDMS from SCCO ₂	28
13.	MECs of various TiO ₂ particles tested with SRI nozzle in 190 m ³ chamber	31
14.	MECs of SCCO ₂ -dried TiO ₂ particles tested with SRI nozzle in 190 m ³ chamber	31
15.	ED tests in 190 m ³ chamber	32

TABLES

1.	Base Materials for Project (All with individual particles of 0.25 μm)	3
2.	ECBC Benchmark Data	4
3.	Effect of Gas Pressure on Particle Deposition Rate as Fraction of Total Mass Deposited: As-Received Tiona 188 as a Percentage of Total Samples Collected on Papers	8
4.	Settling Rate for the Base Materials (As Received)	9
5.	Dry Particle Size Measurement	11
6.	Particle Size Comparison with Army Data	11
7.	Moisture Content and Settling Time of As-Received TiO_2 Powders	12
8.	Thermal Drying (110 $^{\circ}\text{C}$) vs As-Received Powders	13
9.	Drying of TiO_2 Particles in SCCO_2	14
10.	Extraction/Drying with CO_2 /Polar Molecule Mixtures	15
11.	Scale-Up of Drying from 1 to 15 g Batches	16
12.	Calculated MECs from Small Chamber Obscuration Tests at NanoComposix	17
13.	Drying of TiO_2 Particles with Agitation in SCCO_2	21
14.	RCL-9/DPDMS Storage at Different Humidities	22
15.	RCL-9/DPDMS Moisture and Aerosolization vs Benchtop Storage Time in MVTR of 0.02 g/100 in. ² per day.....	25
16.	Settling Time after Storage	26
17.	Effect of Exposure to Humidity on Moisture Content of TiO_2 Powders: MVTR = 0.005 g/100 in. ² per day	26
18.	Coating RCL-9 DPDMS	27
19.	Coating RCL-9 with DPDMS and FS from SCCO_2 with and without Agitation	29

FINAL REPORT:
STORAGE DEVICE/PACKAGE FOR TITANIUM DIOXIDE PARTICLES

1. INTRODUCTION

1.1 Background and Objectives

1.1.1 Visible Obscuration with TiO₂ Particles

The U.S. Army uses numerous target defeat technologies to protect Army personnel and equipment from the adversary. A TiO₂ particle cloud, dispersed by a grenade's detonation, is one of the few methods the individual Soldier has of "instantaneously" creating visible obscuration in field operations. The radius of the obscured zone from an individual TiO₂ grenade is small and, in practice, generally lasts less than a minute or two. The army is interested in improving the obscuration characteristics of TiO₂ by increasing the dispersion characteristics of the powders. Additionally, the Army has been advised by its current sole supplier of the TiO₂ for these grenades that it no longer wants to produce these materials for this application.

The U.S. Army currently uses pigment grades of TiO₂ particles as visual obscurants. These are in predominantly the rutile form of the material, which is the preferred form because of the higher density and refractive index. These particles are nominally 0.25 μm in diameter, have been rendered hydrophobic by surface treatment with an organosilane, and are packed into grenades for dissemination by explosive detonation. The released particles serve as obscurants in the visible light wavelength range.

The grenades do not perform as well as expected, i.e., the suspension time of the particles in air is reduced below the expected theoretical, due to several factors. The factors causing reduced performance include (a) incomplete dissemination of the particles from grenades, (b) agglomeration of particles prior to use in filling the grenades, (c) agglomeration of particles because of compression within the grenades, (d) and perhaps, particle agglomeration caused by detonation.

The reduced performance of the grenades decreases the time period over which the white cloud from TiO₂ particles can create sufficient obscuration to protect people and equipment involved in an operation behind this smoke. The U.S. Army is interested in increasing the suspension time of particles in the air to allow longer times for protection.

1.1.2 Figure of Merit

The performance of the obscurant is measured as a figure of merit (FoM), which is a function of material properties and the dispersion created by the detonator in the grenade.

$$\text{FoM} = (\alpha)(\rho_{\text{fill}})(\text{Yield}) \quad (1)$$

where

α = mass extinction coefficient (MEC) in square meters per gram (m^2/g), which increases with the material refractive index and varies with the particle diameter and the wavelength of the electromagnetic radiation

ρ_{fill} = bulk density of material in grams per cubic centimeter (g/cc) multiplied by the fill volume fraction of the grenade

Yield = ratio of material airborne to initial amount of material in grenade

In general, the Army would like to both increase the obscuration level and extend the particulate-settling time. Ideally, better obscuration would be accomplished with the same weight load of TiO_2 or the same obscuration would occur with less TiO_2 weight. Extending the duration of obscuration from a given weight load of TiO_2 would be accomplished by extending the settling time of the particulates.

Data gathered by the Army on the dispersion of various surface-treated TiO_2 particles shows that for a material of a given particle size and density, the FoM is largely controlled by the extinction coefficient in the visible spectrum wavelength range and the yield of particles caused by the detonation of the grenade. These two parameters are strongly affected by TiO_2 particle agglomeration. Larger agglomerates (larger than the wavelength of light) result in:

- (a) an increase in the mass per particle (agglomerate);
- (b) a decrease in the number of potential particles (scattering sites) per grenade load, resulting in a decrease in *Yield*;
- (c) a more rapid fall of the particles (agglomerates) from a suspended state; even to the extent that the large agglomerates fall immediately to the ground and are thereby eliminated, which decreases *Yield* and FoM; and
- (d) a decrease in α , thereby reducing the FoM.

Yield is additionally affected during detonation by the coupling of energy to the TiO_2 particles to cause particle suspension in air. Nonuniform energy coupling results in a significant number of particles simply falling to the ground, thereby reducing *Yield* in eq 1.

Thus, the charter of this work was to increase particle dispersion as a means of increasing both *Yield* and α .

1.1.3 Materials Investigated and Base Performance

The current material (at the time of this report) used in grenades was TiO₂ with nominal 0.25 µm (250 nm) particles. These particles were treated with an organosilane to increase the surface hydrophobicity of the TiO₂ particles to decrease particle agglomeration.

As described in the proposal for this project, some particle agglomeration is caused by the adsorption of water vapor or solvent on the particle surfaces during and after particle surface treatment, which involved coating the particles with a solution of the organosilane in an alcohol (Hobbs and Anand, 2009). (Note: Surface tension associated with the adsorbed liquids is a cause of agglomeration.) Thus, the major approaches to reducing the particle agglomeration were by (a) drying the particles in supercritical carbon dioxide (SCCO₂) with zero surface tension, (b) coating the as-procured, untreated TiO₂ particles with fluorosilane from SCCO₂, and (c) after drying, packaging the treated particles in barrier packages to reduce uptake of moisture, thereby limiting post-drying agglomeration.

The focus of the project was on drying and coating four different TiO₂ particles; these are noted in Table 1:

Table 1. Base Materials for Project

Material (All with individual particles of 0.25 µm)	Treatment	Provided by
CR 470	Organosilane	U.S. Army Edgewood Chemical Biological Center (ECBC)
Tiona RCL-9	None; inorganic surface	ECBC (from Millenium Inorganic Chemicals, Glen Burnie, MD)
Tiona RCL-9	Coated with diphenyldimethoxysilane (DPDMS)	ECBC
Tiona 188	Proprietary hydrophobic surface treatment	Halide Group, Inc. (HGI) (from Millenium Inorganic Chemicals)

RCL-9 was selected as the base hydrophilic material for coating with DPDMS and fluorosilane from SCCO₂.

The four TiO₂s noted in Table 1 were characterized by the Army using numerous techniques including particle size and distribution, which were measured using particle size analyzers. Obscuration effectiveness was measured in the 190 m³ chamber with both the Stanford Research Institute (SRI) nozzle and explosions of grenades. The obscuration testing revealed the overall performance FoM, particle extinction coefficient, and yield of small particles that remained suspended to cause obscuration. The data from the report issued by Dr. Brendan

DeLacy from the ECBC are summarized in Table 2 (DeLacy et al., 2011). These data serve as the benchmark for comparison.

Table 2. ECBC Benchmark Data

TiO₂ Designation*	Extinction Coefficient (SRI nozzle)+	Calculated Particle Size (SRI) (μm)	Extinction Coefficient (ED)#	Particle Yield (ED)	Calculated Particle Size (ED) (μm)	FoM (ED)	Median Diameter (D₅₀) μm**
CR 470	3.79	1.6	2.10	0.31	7.1	0.63	0.9
Tiona 188	4.26	2.1	1.97	0.14	7.3	0.34	1.2
RCL-9	3.35	1.6	1.11	0.15	7.4	0.19	1.6
RCL-9/ DPDMS	4.07	2.7	2.46	0.30	5.4	0.94	0.7

* All are nominal 0.25 μm TiO₂ particles

+ Yield of particles >0.90; yield is a measure of initial particles that are aerosolized

Explosive dissemination (ED)

** Measured by laser light diffraction; a powder disperser is used in the Sympatec particle size measurement equipment (Sympatec, Clausthal-Zellerfiend, Germany)

The data in Table 2 show:

- (a) Poor correlation in particle obscuration performance as measured and calculated by the two procedures, SRI nozzle and explosively disseminated (ED) particles.
- (b) A significant difference in the calculated particle sizes (based on particle-settling time) between SRI nozzle dissemination and ED, i.e., ED is not as effective as the SRI nozzle.
- (c) A very low yield of particles by ED, compared with >90% obtained using the SRI nozzle (making SRI nozzle appear more effective).

ECBC has also measured the rheological and mechanical properties of the TiO₂ particles. No correlation has been identified between these measurements and the FoM in the obscuration achieved during grenade testing. It appears from the data in Table 2 that the FoM was affected primarily by the coupling of the explosive energy from a grenade to the TiO₂ particles. The apparently large particle size, calculated from the ED testing, suggests that (a) there may be a possible fusion of particles during the explosion, (b) particle agglomeration may occur as a result of packing the grenade with TiO₂ particles, or (c) there may be a nonuniform coupling of energy between the explosion and the particles, which is a possibility supported by the low yield of particles that are aerosolized by the explosion.

Thus, the behavior of the visual obscuration caused by TiO₂-filled grenades was not well understood. Some of the work in this project was directed toward a better understanding of the process, although this was not the main objective of this project.

Project Tasks

The detailed deliverables (tasks) for the project were as follows:

- Set up laboratory FoM characterization tools:
 - Design and build laboratory powder aerosolization tester
 - Procure and start up Karl Fischer moisture analyzer (Hanna Instruments, Smithfield, RI) to measure moisture content on powder sample surfaces
 - Outsource particle shear strength measurement
 - Conduct particle size analysis
 - Use HORIBA Scientific particle analyzer (at vendor location)
 - Perform in Army labs
 - Install and adapt the Applied Separations (Allentown, PA) equipment for SCCO₂ moisture extraction and dry handling
- Drying of particles:
 - Dry thermally at >100 °C (Section 2.4)
 - Dry with SCCO₂ (Section 2.5)
 - SCCO₂ scale up to larger samples
 - Different SCCO₂ conditions—temperature, pressure, additives in SCCO₂
- Develop and test packaging to maintain dryness of TiO₂ particles (Section 2.0):
 - Test the effects of humidity on particle performance (Section 2.1)
 - Evaluate kinetics of moisture uptake (Section 2.1)
 - Develop criteria for packaging of TiO₂ particles (Section 2.2)
- Coat particles in SCCO₂ and test performance:
 - Coat particles with DPDMS (Section 2.6)
 - Coat particles with fluorosilane (Section 2.7)
- Perform ECBC testing of dried and coated TiO₂ powders (Section 2.5)
- Evaluate smaller primary particle TiO₂ materials in obscuration testing (Section 2.8) and conduct tests in Army 190 m³ chamber (Section 2.8)
- Analyze deagglomeration of TiO₂ particles under shear (task added, not in proposal)

2. SET UP LABORATORY FOM CHARACTERIZATION TOOLS

2.1 Aerosolization Testers

The initial design of the aerosolization chamber is shown in Figure 1, with the laser pointer held at the level of the red line.



Figure 1. Laboratory FoM aerosolization tester.

A small sample, approximately 0.1 g of TiO_2 particles, was placed inside a nozzle and a fixed volume of gas at a fixed pressure (10 psig) was used to aerosolize the particles as they emerged from the nozzle. The time required for all the particles to settle was measured (settling time). The particle-settling endpoint was detected by pointing a laser light across the bottom of the aerosolization chamber at approximately 1 in. above the base. If particles were present, the Tyndall effect caused a scattering of light from the particle surfaces and made the particles glow with the color of the laser light. The endpoint, when all the particles were settled, was easily determined.

Using the fundamental settling equation (reference the monthly report from January 2011), the settling time was determined to be inversely proportional to the square of the particle diameter. Thus, larger particles would be expected to settle faster than smaller particles. Figure 2 shows the calculated settling times for TiO_2 particles as a function of particle diameter in the aerosolization chamber. (Note: At 10 psig across the nozzle, the maximum height of particles was ~20 in.; some particles may have impacted the filter paper at the top of the tester.)

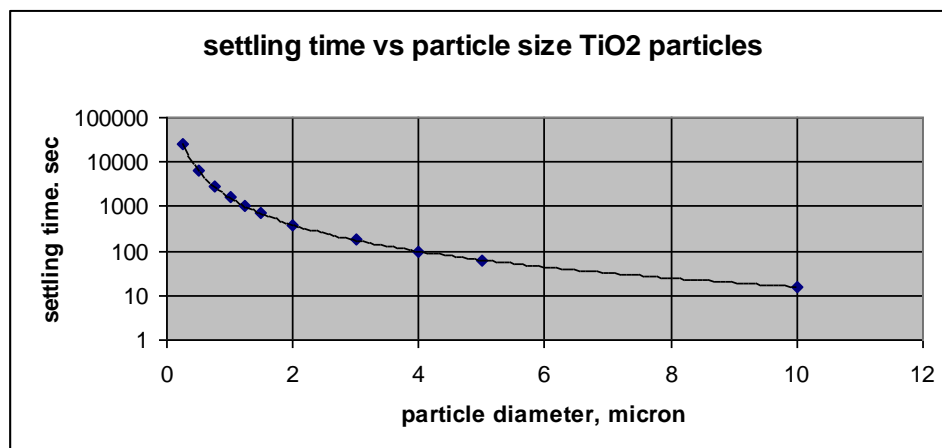


Figure 2. Calculated settling times for TiO_2 particles as a function of particle diameter, where the desired particle size is $0.25 \mu\text{m}$.

It became apparent that a large (mass) fraction of the particles settled very quickly (i.e., tens of seconds for particle sizes $>10 \mu\text{m}$), although some particles (readily detectable by the Tyndall effect) took 10 min to 1–3 h to settle. Thus, we concluded that the endpoint, test results were biased by the smallest particles and were not representative of the behavior of the bulk of the particles or the obscurant effect. In obscurant applications, obscuration is most effective when more particles are aerosolized (i.e., the number of appropriately sized particles in the obscurant volume are large).

The aerosolization equipment was modified to measure particle settling over the first 120 s to understand the effectiveness of the test sample as a practical obscurant. This was done by measuring the weight of particles that settled at the bottom of the aerosolization chamber over small time intervals. In addition, in this apparatus, the diameter of the plastic chamber was increased, and the pressure drop across the nozzle was increased from 10 to 50 psi. Increasing the pressure drop across the nozzle increased the yield of smaller particles and allowed the settling test to be stretched over longer test periods. Table 3 shows the typical settling times as a function of pressure for Tiona 188.

Table 3. Effect of Gas Pressure on Particle Deposition Rate as Fraction of Total Mass Deposited: As-Received Tiona 188 as a Percentage of Total Samples Collected on Papers

Pressure (psig)	Aerosolization Time from Tyndall Effect Endpoint (min)	Particles Deposited Between 0 and 0.5 min	Particles Deposited Between 0.5 and 1 min	Particles Deposited Between 1 and 1.5 min	Particles Deposited Between 1.5 and 2 min
5	3.37	100.0	0.0	0.0	0.0
10	11.43	75.2	14.9	4.0	5.9
15	31.63	74.0	16.7	7.3	2.1
20	47.42	77.1	12.0	9.6	1.2
25	47.02	69.4	9.7	11.1	9.7
30	51.92	79.1	9.0	9.0	3.0
35	47.72	71.1	15.8	9.2	3.9
40	66.09	67.2	17.9	13.4	1.5
45	120+	47.7	22.7	22.7	6.8
50	120+	62.9	14.3	14.3	8.6

The data show:

- (a) As the pressure drop across the nozzle increased, the yield of the smallest particles increased, as manifested by the settling times (endpoint measured with laser device). The maximum pressure that could be used was limited by the stability of the plastic nozzle and the maximum height the particles could reach without leaving the aerosolization chamber from the top.
- (b) The percentage of the particles that had the shortest settling times decreased as the pressure drop across the nozzle increased. The higher pressure also seemed to increase the fraction of particles that settled at longer times, although the effect was not dramatic in this pressure range (5 to 50 psig).

Thus, gas at 50 psig pressure was used in the modified test protocol to evaluate the aerosolization characteristics of the powders after drying and surface treatment. The settling rates for the three base surface-treated TiO_2 s (without drying) are shown in Table 4. Analysis of the data suggest that of the three materials, RCL/DPDMS had a greater mass of TiO_2 that remained suspended longer. These data were in general agreement with the benchmark data reported by the Army (Table 2). In addition, evaluation of the data also indicated that the bulk of the obscuration achieved with these particles lasted about 60–120 s. This time was within the range of typical visual obscuration grenades that use TiO_2 as the obscurant.

Table 4. Settling Rate for the Base Materials (As Received)

Material	Settling Times (s)			
	0–30	31–60	61–90	91–120
	Material Collected on Sample Collection Disks (% of total)			
RCL/DPDMS	46.2	15.4	30.8	7.7
Tiona 188	62.9	14.3	14.3	8.6
CR 470	81.8	4.5	9.1	4.5

2.2 Karl Fischer Moisture Analysis

A Karl Fischer moisture analyzer was procured and installed to measure the moisture content of the powders. Figure 3 shows the moisture analyzer.



Figure 3. Moisture analyzer set up in the lab.

The moisture analyzer consisted of three main components:

1. The sample drying system, which could be programmed to the desired temperature for removal of water from the sample;
2. The titration part of the apparatus, which titrated all the moisture released from the sample; and
3. The programming and data-handling system.

In the screening experiments done on the system, it was determined that a minimum of 0.1 g of the TiO_2 powder was required to measure the moisture content reproducibly and accurately. Thus, all TiO_2 particle drying data were generated using a sample size of at least 0.1 g.

2.3 Particle Shear Strength: Unconfined Yield Strength

Unconfined yield strength of particles is a measure of the flow properties of powders; this technique is often used to understand flow of particles in a hopper. A new shear strength spin tester (Material Flow Equipment, Gainesville, FL) is capable of characterizing particle flow properties using a very small sample (0.05 g). The principal of this instrument is similar to that for a uniaxial shear cell. The instrument measures the centrifugal force needed to compact the sample and then the force required for failure of the solids, thereby measuring the yield strength.

The equipment consists of a horizontal center rotor with an attached arm. At the end of the arm a very small, vertically oriented, conical microhopper is attached with the hopper's larger opening on the top. Both the top and the bottom of the hopper have removable covers. In the first step of the evaluation, the hopper was filled with the powder, and the arm was rotated at a fixed number of revolutions per minute (rpm) setting with the covers on (note, rpm variation allows consolidation at different forces). The centrifugal force causes consolidation and/or compression of the particles. Once the powders are consolidated, the top and bottom of the hopper are opened, and the rotation speed is ramped up until the powder flows out of the bottom of the microhopper. The rotation speed, arm length, and powder sample mass enables calculation of the stress at which powder flow occurs (unconfined yield strength). Lower yield strength typically implies less resistance to the initiation and flow of powders.

The four main TiO_2 powders used in this study were tested as received and after drying at 110 °C. The data and details are shown in Appendix A.

The main conclusions were:

1. The test measured different yield strengths for the four basic TiO_2 forms with individual particles $\sim 0.25 \mu\text{m}$ in diameter.
2. CR 470 had the lowest yield strength.

3. Heat treatment of particles at 110 °C reduced the yield strength.
4. There was no clear correlation between the ED FoM and yield stresses measured for different TiO₂ particles.

Overall, we think this device provided limited insight into the aerosolization behavior of particles, and the effort was abandoned.

2.4 Particle Size Characterization with Light Diffraction

Analysis of the four base TiO₂ materials was performed using a Horiba laser light diffraction device (Partica LA 950). The results are shown in Table 5 and compared with the data generated by DeLacy et al. in Table 6 using a Sympatec dry particle analyzer.

Table 5. Dry Particle Size Measurement

Material	D10 (μm)	D50 (μm)	D90 (μm)
Tiona 188	0.161	0.281	0.568
CR-470	0.168	0.277	0.549
RCL-9	0.167	0.289	0.617
RCL-9/DPDMS	0.147	0.259	0.463

Note: The median corresponds to D50, 10% of the population lies below D10, and 90% of the population lies below D90.

Table 6. Particle Size Comparison with Army Data

Material	D50 (μm)	D50 (Army) (μm)
Tiona 188	0.281	1.21
CR-470	0.277	0.9
RCL-9	0.289	1.6
RCL-9/DPDS	0.259	0.7

Note: The last column in Table 6, D50 Army was extracted from the report by DeLacy et al., 2010.

The data were surprising because the D50 values (median particle size) measured on the four standard materials were almost identical and very close to the inherent particle size of the TiO₂. This was not consistent with the data generated by the U.S. Army. Evaluation of the data in Table 5 also indicated that the nozzle used to disseminate the particles into the analyzer chamber coupled sufficient energy into the particles to break them apart. This concept was investigated further as described in Appendix B of this report.

2.5 Adaption of Applied Separations SCCO₂ Equipment

Initial sample-drying experiments were carried out using a standard 24 mL extraction vessel and SCCO₂ extraction system obtained from Applied Separations. However, for scale-up beyond the initial 1–2 g samples, larger systems were required at 100 mL for 15 g samples and 500 mL for 50 g samples. In addition, for the DPDMS and fluorosilane coating from SCCO₂, dual-vessel systems were assembled.

It also soon became apparent that because of the TiO₂ performance changes observed with drying (discussed in Section 3.2), it was necessary to install a dry box that was outfitted with glove ports and an airlock. This was needed to transfer the SCCO₂ dried materials and enable the performance of the dry powder Karl Fischer analysis. The purchased glove box was neither airtight nor moisture-proof. However, it was possible, under a light-positive dry nitrogen purge, to maintain a relative humidity (RH) of ~8% while working, compared with ~30% in the general laboratory space. This proved adequate for the study of RH exposure on performance.

3. DRYING OF TiO₂ PARTICLES WITH SCCO₂ AND BY THERMAL TREATMENT

The main objective of the project was to dry surface-treated TiO₂ particles with SCCO₂. It is well known that SCCO₂ has a low surface tension and very low polarity. As a consequence, SCCO₂ has good solubility for hydrocarbons and fluorinated molecules, but low solubility for H₂O. Interestingly, the polarity of the SCCO₂ can be altered by (a) increasing the temperature of SCCO₂ and (b) incorporating small amounts of polar solvents (e.g., methanol, ethanol, and acetone) into SCCO₂.

TiO₂ powders were dried under different supercritical conditions. After drying, the moisture content and the settling time of the TiO₂ powders were measured in the aerosolization chamber (using laser endpoint detection). The dried particles were stored and handled in the glove box. The steady-state humidity after continuous purge was about 8%. The moisture content of the as-received TiO₂ particles was measured to set up a benchmark; the average data are summarized in Table 7.

Table 7. Moisture Content and Settling Time of As-Received TiO₂ Powders

Material	H ₂ O As Received* (%)	Average Settling Time (s)
CR 470 (hydrophobic; organosilane)	0.351	395
RCL-9 (hydrophilic; alumina coating)	0.703	112
RCL-9-DPDMS (hydrophobic, organosilane)	0.428	413
Tiona 188 (hydrophobic; organic)	0.278	696

* Measured using a Karl Fisher titrator, heated to 110 °C in the moisture analyzer oven.

3.1 Thermal Drying of TiO₂

Benchmark data were developed for thermal drying to compare it with SCCO₂ drying. A drying temperature in excess of 100 °C was assumed necessary, even in the presence of a dry nitrogen sweep gas, due to the sorptive nature of the TiO₂. Excessive temperatures have the potential to degrade the materials, particularly surface coatings. Table 8 summarizes the effects of thermal drying on the moisture content and settling time.

Table 8. Thermal Drying (110 °C) vs As-Received Powders

Material	H₂O As Is* (%)	H₂O After Drying at 110 °C (%)	Average Settling Time As Received (s)	Average Settling Time After 110 °C Drying (s)
CR 470	0.351	0.20	395	730
RCL-9	0.703	0.461	112	286
RCL-9-DPDMS	0.428	0.348	413	122
Tiona 188	0.278	0.207	696	769

Evaluation of the data showed that drying at 110 °C in an oven reduced the moisture content of the TiO₂ particles. There was a concomitant increase in the settling time, except for the case of RCL-DPDMS, which indicates that thermal drying had a beneficial effect on reducing particle agglomeration and increasing the settling time for most of the samples, but may have caused the RCL-9-DPDMS material to agglomerate.

3.2 SCCO₂ Drying of TiO₂

The TiO₂ powders were dried in SCCO₂ at 1500 psig and 120 °C (conditions were chosen based on prior experience). Initially, 1 g of sample was dried in a 24 mL reactor in a batch mode. The sample was held in SCCO₂ for 1 h under static conditions, followed by purge with SCCO₂ for 2 h. The particles were held in a pouch prepared from cellulosic filter paper (opening about 5 µm). In addition, the particles were handled at ambient conditions (~30% RH) or in the glove box at ~8% RH. The typical moisture content and settling times are shown in Table 9.

Table 9. Drying of TiO₂ Particles in SCCO₂

Material	Typical Moisture After Standard SCCO₂ Drying with Ambient Exposure (%)	Moisture After Standard SCCO₂ Drying in Glove Box (%)	Typical Aerosolization, Settling Time with Standard SCCO₂ Drying at Ambient Conditions (s)	Aerosolization, Settling Time with Standard SCCO₂ Drying in Glove Box (s)
CR-470	0.297	0.06	924	1387
Tiona 188	0.268	0.146	900	961
RCL-9/ DPDMS	0.367	0.086	1405	3030

The data in Table 9 show that:

1. Moisture content was reduced very significantly after drying in SCCO₂.
2. Low moisture level was maintained if the particles were handled in the glove box.
3. Particle settling time increased substantially after SCCO₂ drying, especially for RCL-9 particles coated with DPDMS by the Army.

It can also be concluded from evaluation of the data in Tables 8 and 9 that SCCO₂ drying is more effective than thermal drying in reducing particle agglomeration, hence increasing particle settling time. The temperature, pressure, and purge times were varied, but the results were not substantially different from those shown in Table 9 for SCCO₂ extraction alone.

The TiO₂ particles were also extracted separately under more polar SCCO₂ conditions. Table 10 shows typical results from extractions using mixtures of CO₂ with polar cosolvents.

Table 10. Extraction/Drying with CO₂/Polar Molecule Mixtures

Sample	Solvent	Moisture Content of Powder (%)	Settling Time (s)
Tiona 188	SCCO ₂	0.125	734
	SCCO ₂ /MeOH	0.146	961
	SCCO ₂ /acetone	–	363
RCL-9/DPDMS	SCCO ₂	0.086	3030
	SCCO ₂ /MeOH	0.224	1574
	SCCO ₂ /acetone	0.114	3168
CR 470	SCCO ₂	0.06	1387
	SCCO ₂ /MeOH	0.125	882
	SCCO ₂ /acetone	0.099	1335
RCL-9	SCCO ₂	0.224	633
	SCCO ₂ /MeOH	0.18	941
	SCCO ₂ /acetone	0.23	596

Evaluation of the data above show that with the possible exception of the untreated hydrophilic RCL-9 powder, there was no benefit to including a more polar molecule with CO₂ to improve the drying of the TiO₂ particles. Thus, for this study, all additional work was continued with SCCO₂ alone.

3.2.1 Scale-Up of SCCO₂ Drying of TiO₂

The process for drying TiO₂ was increased from 1 to 15 g batches. The scale-up was considered successful according to our qualification procedure for moisture content and aerosolized particle settling time and as shown in Table 11.

Table 11. Scale-Up of Drying from 1 to 15 g Batches

Material	Sample Size (g)	Moisture Content (%)	Settling Time (s)
Tiona 188	1	0.268	901
	15	0.216	1301
CR-470	1	0.108	1382
	15	0.152	1051
RCL-9/DPDMS	1	0.221	3162
	15	0.196	3261

Analysis of the data show that SCCO₂ drying was effective in reducing the moisture content of the TiO₂ particles and increasing the settling time from about 400 s for as-is RCL-9 coated with DPDMS to >3000 s after SCCO₂ drying. This was considered a very significant improvement. RCL-9 coated with DPDMS was also found to have the best performance in the ED tests conducted by ECBC.

Fifteen grams of each of the above materials was packaged in the glove box into the barrier packaging developed for this project and shipped to the Army for testing. The particle performance as an obscurant was tested in the 190 m³ chamber by disseminating the powder into the chamber using an SRI nozzle. From the obscuration created in the chamber, an MEC was calculated. The MEC is a measure of the visual obscuration effectiveness of the particles. Theoretically, MECs for TiO₂ particles can approach 12.0, but typically the MECs have been calculated to be in the range of 4 to 5 using the nondried particles. The results from the Army testing of the SCCO₂-dried TiO₂ particles are shown in Figure 4. The data in Figure 4 show that the MECs of the SCCO₂-dried particles were comparable to those measured using nondried particles. This was surprising because the finding was not consistent with the measurements from our aerosolization chamber, where we measured a greater than sixfold improvement in settling time using RCL-9/DPDMS.

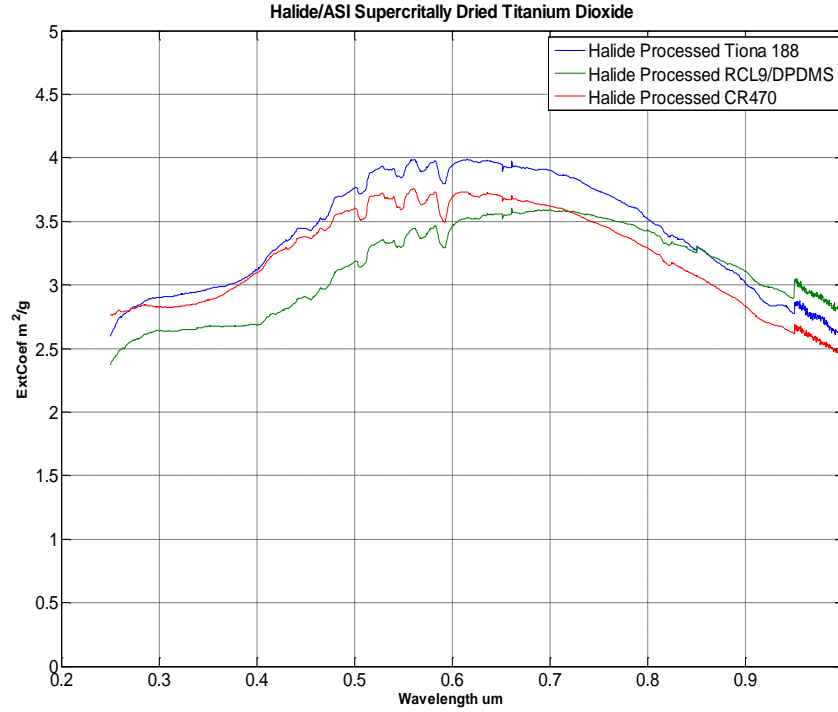


Figure 4. MECs measured from the 190 m³ chamber with the use of the SRI nozzle.

To confirm these findings, we submitted a 1 g SCCO₂-dried sample to NanoComposix (San Diego, CA) for obscuration testing in their small chamber fitted with an SRI-type nozzle. The results are shown in Table 12 and Figures 5 and 6.

Table 12. Calculated MECs from Small Chamber Obscuration Tests at NanoComposix

	Maximum MEC reported by DeLacy	Maximum MEC (400 – >1000 nm)	Maximum Wavelength (400 – >1000 nm)	Average MEC (400 – >1000 nm)	Average MEC (400 – >700 nm)	Average MEC (700 – >1000 nm)
RCL-9 SCCO ₂ -dried [avg]		3.0	604.3	2.5	2.8	2.2
RCL-9/DPDMS as-is [avg]	4.07	3.6	613.3	2.9	3.3	2.6
RCL-9/DPDMS SCCO ₂ -dried [avg]		4.2	607.7	3.4	3.9	3.0
Tiona 188 SCCO ₂ -dried [avg]		4.2	560.8	3.2	3.9	2.6
Tiona 188 SCCO ₂ -dried; 15 g [avg]		4.4	583.1	3.6	4.2	3.1
Tiona 188 reference standard as-received	4.26	3.2	546.5	2.3	2.9	1.8
CR-470 as-is	3.79	4.4	552.6	3.3	4.1	2.6
CR 470 SCCO ₂ -dried [avg]		4.3	546.0	3.3	4.0	2.6

Analysis of the data in Table 12 showed a small improvement in the calculated MECs for the as-is and SCCO_2 -dried TiO_2 particles. These MECs were comparable to those obtained from the 190 m^3 Army chamber tests. NanoComposix personnel also characterized the aerosolized particle size distribution, and these results are shown in Figures 5 and 6. Figure 5 shows the particle size distribution for the various TiO_2 particles. RCL-9/DPDMS samples have the highest yield of the small particles. The data in Figure 6 show the yield of large particles. In this case, the RCL-9/DPDMS samples had the smallest yield of large particles. Both of these observations indicated that testing RCL-9/DPDMS samples should result in the longest settling time in the aerosolization chamber, which was, in fact, observed. Thus, in part, the data were consistent with performance measurement in our aerosolization chamber.

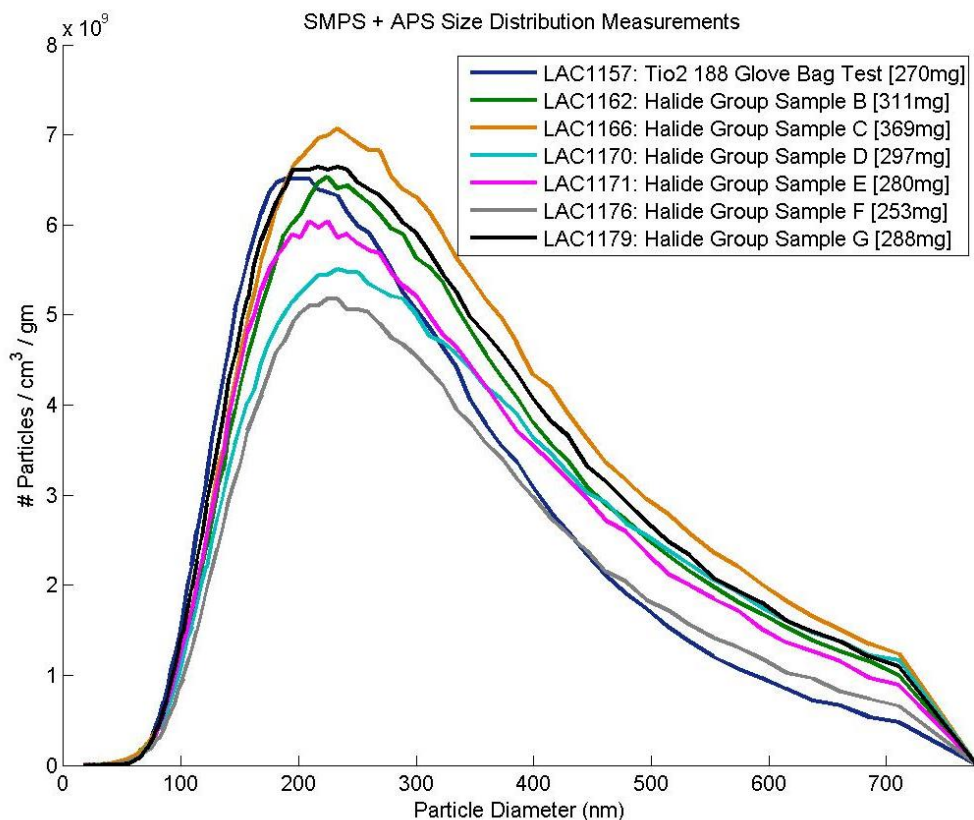


Figure 5. Particle size and yield of small particles in NanoComposix obscuration chamber.

Samples were identified as follows:

B = DPDMS as is
 C = DPDMS/ SCCO_2
 D = CR 470/ SCCO_2
 E = Tiona 188 SCCO_2
 F = RCL-9/ SCCO_2
 G = Tiona 188/ SCCO_2 /15
 LAC 1157 = Tiona 188 as is

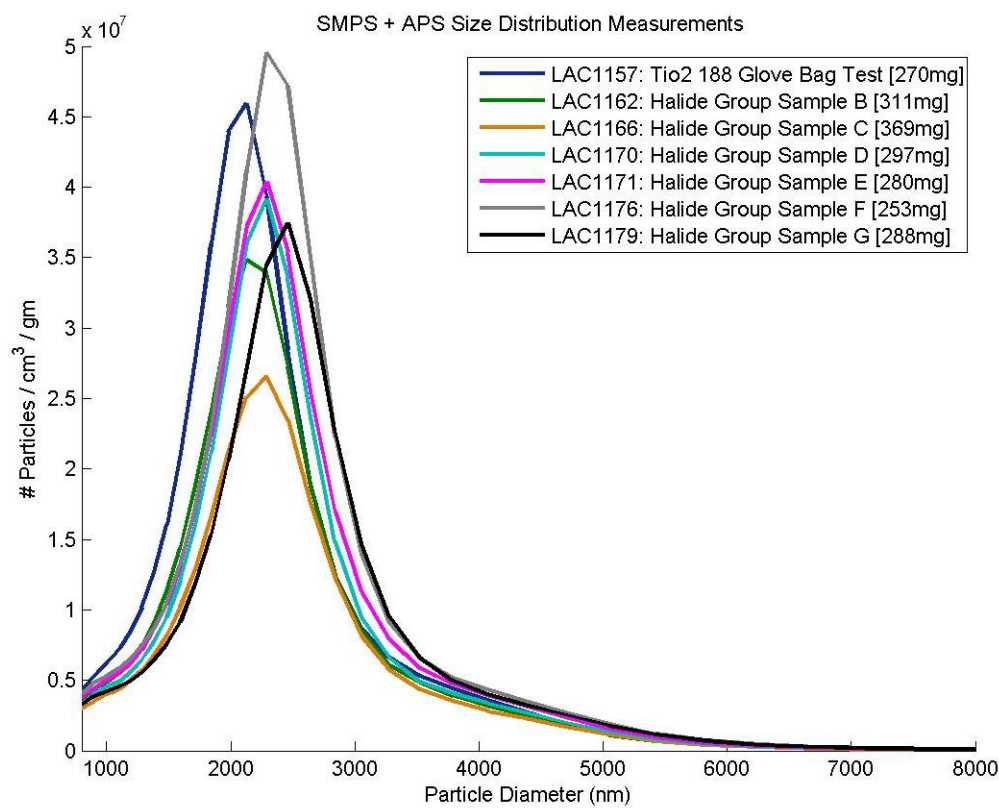


Figure 6. Particle size and yield of large particles in NanoComposix obscuration chamber.

Samples were identified as follows:

B = DPDMS as is
 C = DPDMS/SCCO₂
 D = CR 470/SCCO₂
 E = Tiona 188/SCCO₂
 F = RCL-9/SCCO₂
 G = Tiona 188/SCCO₂/15
 LAC 1157 = Tiona 188 as is

The important conclusions from the results on the dried particles are:

1. When using our in-house aerosolization chamber, the longest settling time was observed with RCL-9 coated with DPDMS (Sample F).
2. The MECs measured during obscuration testing in the small (NanoComposix) and large (U.S. Army) vessels, while disseminating the sample with an SRI nozzle, showed only a small improvement in MEC with SCCO₂ drying.

3. Evaluation of the performance of RCL-9/DPDMS (Sample F) appeared to be the best for visual obscuration.
4. SCCO₂ drying did cause the formation of more small particles, but the amount of additional small particles obtained was small, which did not significantly increase visual obscuration.
5. The laboratory aerosolization tester, which measures the settling time with the laser detector, was strongly influenced by the presence of small particles. Thus, even a small fraction of small particles increased the settling time tremendously. This could be misleading for the assessment of practical obscuration. Practically, the largest obscuration was obtained when a large mass fraction of the most efficient scattering particles (high α particles) remained suspended in air. When these efficient scattering particles were also the smallest particles in the obscurant cloud, then good scattering required a very large fraction of these particles. Thus, it is important to measure when the largest fraction of the particles are aerosolized, rather than measure the performance based on the remnants of the smallest-sized aerosolized particle. This is especially true if the small particles represent a very small fraction of the particle mass suspended.
6. This study resulted in the development of a new aerosolization test that focused on short-term aerosolization and attempted to measure the mass fraction of the settled particles. The details of this test were described earlier in the report.

3.2.2 SCCO₂ Drying of TiO₂ with Agitation

This study evaluated a new drying technique that would potentially increase the number of small particles in the powder while drying with SCCO₂. This method involved agitation of the particles while exposing them to SCCO₂ so the fraction of agglomerated particles could be reduced. A new vessel was prepared for SCCO₂ treatments with the ability to agitate the particles during drying or coating with an organosilane. The new vessel had a 500 mL capacity (apparatus described in Feb 2011 report). The agitator impeller was a flat blade, which could be moved up and down in the vessel. The vessel could be used for treating larger quantities of the TiO₂ powders. RCL-9/DPDMS-coated (by Army) TiO₂ particles were dried with agitation in the new reactor setup. Previous drying work was done without agitation. The samples were analyzed for moisture content and short-time aerosolization (i.e., settling rates). The results are summarized in Table 13.

Table 13. Drying of TiO₂ Particles with Agitation in SCCO₂

Processing Conditions			Aerosolization Results				
Material	Rotation Speed (rpm)	Moisture After Drying (%)	Recover in 30 s (%)	Recover in 60 s (%)	Recover in 90 s (%)	Recover in 120 s (%)	Settling Time (min)*
RCL-9/DPDMS	800	0.258	50.0	25.0	16.7	8.3	54.1
RCL-9/DPDMS	550	0.29	64.7	23.5	11.8	0.0	58.3
RCL-9/DPDMS	0	0.221	46.8	23.9	18.3	11.0	58.4

* Settling time determined as the end of Tyndall effect when using laser light

Evaluation of the data in Table 13 did not show a significant difference in the moisture content and short-time aerosolization behavior of the samples dried by agitation when compared to the control samples dried without agitation. No further effort was expended on optimizing the use of agitation of particles during drying with SCCO₂.

4. DEVELOP AND TEST PACKAGING FOR TiO₂ PARTICLES

The first step in the project was to develop a storage device/package for the TiO₂ particles so the dried particles could be kept dry. Although glass storage was not practical, it was assumed that dried TiO₂ particles, stored in sealed glass vessels under nitrogen or along with desiccants, should neither gain nor lose moisture. There was no evidence found in the literature to determine that oxygen contributes to TiO₂ particle agglomeration. Hence, the focus was primarily on the control of moisture intrusion into the TiO₂ storage package. The basic premise was that moisture leads to increased particle agglomeration, thereby reducing particle aerosolization and subsequently reducing obscuration capability.

4.1 Baseline Data on Water Vapor Adsorption

RCL-9 coated with DPDMS was used as a benchmark to demonstrate the effect of moisture exposure to aerosolization. The coated particles, as received from the Army, were exposed to 3.7, 30, and 75% humidity for up to 2 weeks. Table 14 shows the effect of exposure on moisture uptake and (endpoint) settling time in the aerosolization chamber.

Table 14. RCL-9/DPDMS Storage at Different Humidities

Humidity (%)	No. of Days on Test	Moisture (%)	Settling Time (s)
3.7	0	0.229	3169
	15	0.223	3389
30	0	0.225	3121
	8	0.228	2705
75	0	0.251	2841
	9	0.518	1531

Evaluation of the data very clearly shows that exposure to 75% humidity increased the adsorbed moisture on the TiO_2 particles. There was a concomitant significant decrease in the settling time that was suggestive of particle agglomeration.

We investigated the effect of moisture uptake on particle aerosolization for the other TiO_2 particles also. Some key representative data are shown in Table 14 for particles dried with SCCO_2 , followed by exposure to varying humidity environments. The adsorbed moisture was reduced after drying with SCCO_2 (which represents data with $\sim 0.2\%$ water). As in Table 14, the data in Figure 7 generally show that as the moisture content of the TiO_2 particles increased, the settling times decreased. A shorter settling time indicates a larger particle, which means more particles have agglomerated.

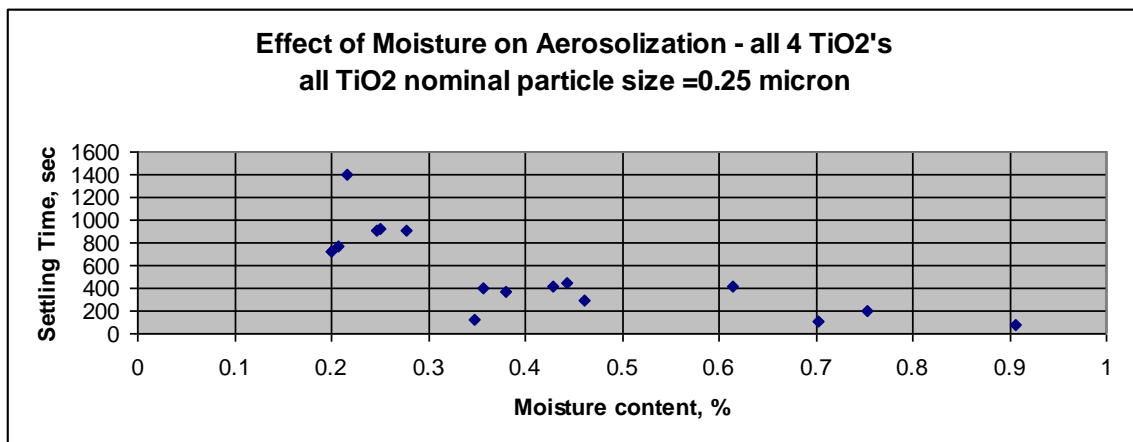


Figure 7. Effect of moisture content on settling time in aerosolization chamber.

From evaluation of these data, it appeared that if the moisture content could be kept below about 0.25%, the aerosolization capability was not affected significantly. Note: if the nominally spherical TiO_2 particles have a diameter of $0.25\ \mu\text{m}$ and a density of $4.2\ \text{g/cc}$, a moisture content of 0.25 wt % would approximately correspond to a monolayer of water on the surface of the TiO_2 particles.

4.2 Moisture Adsorption Kinetics

The rate of moisture uptake by TiO_2 particles was studied to develop the protocol for handling the particles. The data at two humidities, 30 and 8% RH, are shown in Figures 8 to 11 for the four base TiO_2 forms. The 30% humidity represents the laboratory's bench-top environment, and 8% represents moisture in the glove box. The TiO_2 powders were initially dried in the Karl Fischer moisture analysis oven at about 120 °C. The moisture content of these powders was zero at the onset. The powders were then exposed to the two humidities and the moisture uptake rate was measured using the Karl Fischer titrator.

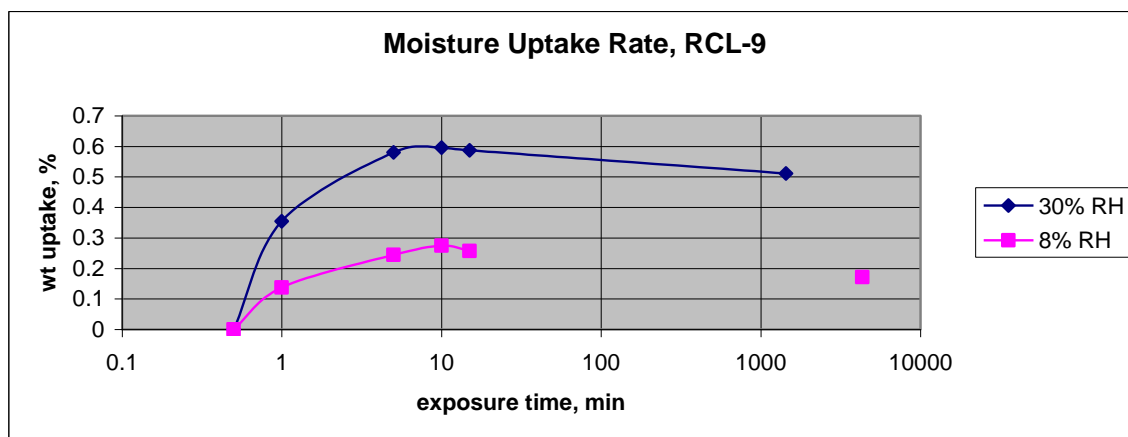


Figure 8. Moisture uptake rate: RCL-9.

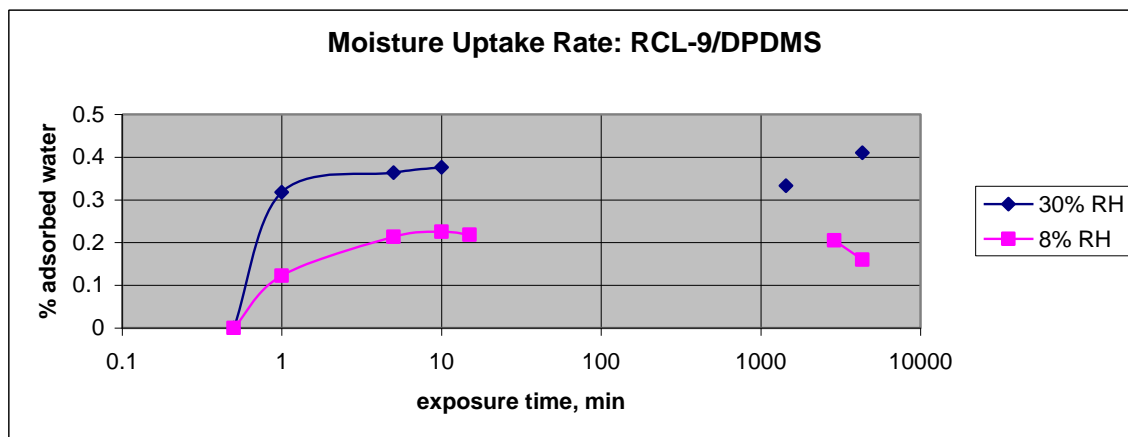


Figure 9. Moisture uptake rate: RCL-9/DPDMS.

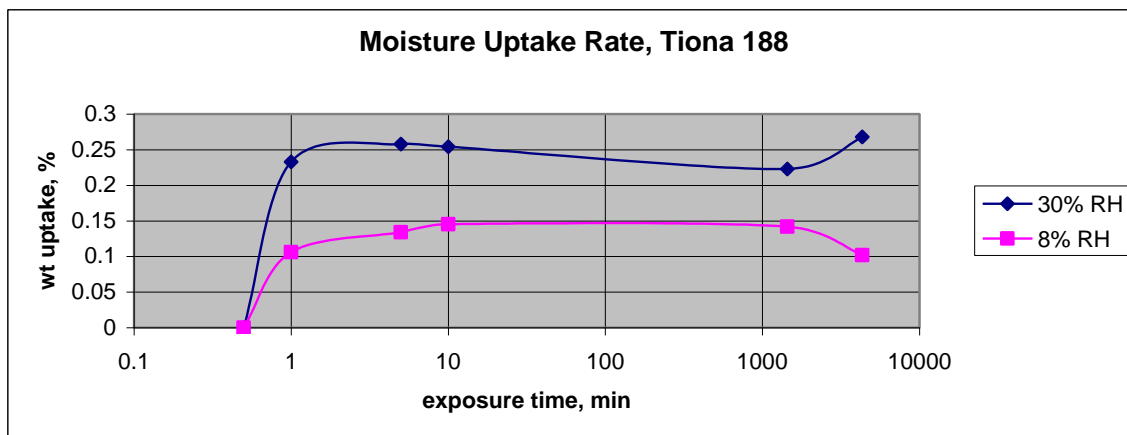


Figure 10. Moisture uptake rate: Tiona 188

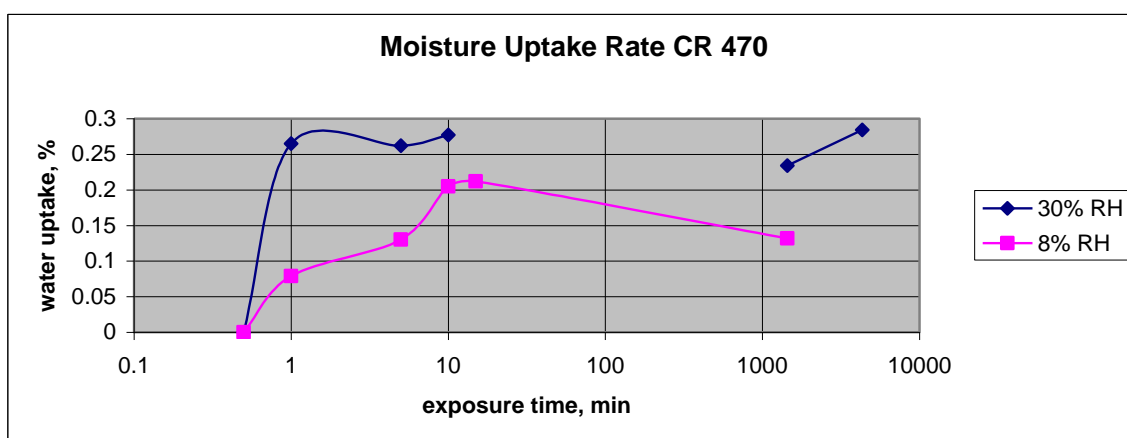


Figure 11. Moisture uptake rate: CR 470

Evaluation of the data in Figures 8–11 shows the following:

1. In small samples, the moisture uptake was rapid, with bulk of the uptake occurring in ~5 min. The moisture uptake equilibrated after about 10 min.
2. As expected, the equilibrium moisture uptake was lower at lower humidity.
3. The highest moisture uptake was for the hydrophilic TiO_2 , the uncoated RCL-9.
4. Handling the samples in the glove box reduced the short-term moisture uptake by >50%.

There was some variability in the data, which is likely related to small fluctuations in ambient and glove box humidity. The important conclusion is that exposure to

ambient humidity should be minimized, and most of the sample-handling and packaging should be done in a dry environment, like the glove box.

4.3 Packaging for Storage of TiO₂ Particles

The as-received TiO₂ particles for this application were packaged in polyethylene bags and enclosed in a card box container. This was not a good moisture barrier system and did not protect the particles from the effects of exposure to high humidity. Different types of commercial packaging were investigated for this application, such as packaging in multilayer moisture barrier bags.

Two multilayer (polymer-metal with interlayer) bags were selected for evaluation of TiO₂ particle storage. One bag had a moisture vapor transmission rate (MVTR) of 0.02 g/100 in.² per day and other with an MVTR of 0.005 g/100 in.² per day. Lower MVTR bags have better moisture barrier properties. In the initial work, TiO₂ samples were stored in the higher MVTR bags. The samples were then placed on a bench top with ~30% RH and in a chamber with 3.7% RH. The samples were periodically removed from the bags and tested for moisture content and aerosolization capability. The data for RCL-9/DPDMS, dried in SCCO₂, packaged in a barrier bag, and stored on a bench top at 30% RH are shown in Table 15.

Table 15. RCL-9/DPDMS Moisture and Aerosolization vs Benchtop Storage Time in MVTR of 0.02 g/100 in.² per day

Storage Time (days)	H₂O Content After SCCO₂ Drying (%)	Settling Time After SCCO₂ Drying (s)
Not Dried, As-received	0.428	–
Initial After SCCO ₂ Drying	0.337	1405*
Day 2	0.404	2011
Day 7	–	1756
Day 11	0.453	1560

*Settling time not measured for this specific batch; value typical for this material after SCCO₂ drying.

Analysis of the data in Table 15 suggests there was a gradual increase in adsorbed moisture on the TiO₂ particles stored in these bags and there may have been a concomitant decrease in the settling time in the laboratory aerosolization test.

Additional tests were conducted by placing the bags containing the TiO₂ particles in a container that was maintained at about 4% RH. The data with various TiO₂ powders is shown in Table 16.

Table 16. Settling Time after Storage

Material	Aerosolization, Typical Settling Time	
	After SCCO ₂ Drying (s)	After SCCO ₂ Drying and ~10 days in Dry Storage (s)
RCL-9	444	881
RCL-9/DPDMS	1405	1777
CR-470	924	787
Tiona 188	900	1000

Evaluation of the data in Table 16 suggested that there was no significant change in aerosolization performance after storage at low humidity conditions. Moisture content of the powders was also measured, and most of the samples had little change in moisture content after these storage conditions.

Since the storage of powders can occur at high ambient humidity conditions, the focus of the subsequent storage studies was on the use of lower MVTR bags. Dried TiO₂ particles of DPDMS-coated RCL-9 were packaged in multilayer moisture-barrier bags. The bags were stored at 3.7, ~30 (ambient laboratory), and 75% humidity. Samples were periodically removed and tested for moisture content and aerosolization performance. The samples have been in storage for >90 days. The last test was performed after 77 days of exposure to moisture conditions as noted. The data from moisture changes are summarized in Table 17.

Table 17. Effect of Exposure to Humidity on Moisture Content of TiO₂ Powders:
MVTR = 0.005 g/100 in.² per day

Sample: DPDMS coated RCL-9 (Army)	Moisture Content (%)	Moisture Content at 3.7% RH Exposure (%)	Moisture Content at 30% RH Exposure (%)	Moisture Content at 75% RH Exposure (%)
As-is, not dried	0.65	—	—	—
Initial after drying, 0 days	0.20	—	—	—
11 days	—	0.23	0.22	0.25
29 days	—	0.22	0.23	0.24
50 days	—	0.21	0.26	0.22
77 days	—	0.26	0.26	0.25

Analysis of the data in Table 17 showed that there was little or no change in the moisture content of any of the particles stored in the moisture-barrier bags. Thus, it appeared that at 75% RH and room temperature, the bags were effective in keeping out moisture.

The samples were also tested using the older and newer aerosolization test protocols. Upon evaluation, the data showed no distinction between the as-prepared and the conditioned samples. Thus, it appeared that the barrier bags, with an MVTR of 0.005 g/100 in.² per day, were adequate for this application.

5. COATING TiO₂ PARTICLES FROM SCCO₂

5.1 DPDMS Coating and Drying of Particles in SCCO₂

Because RCL-9 particles, coated with DPDMS by the U.S. Army, have demonstrated excellent performance during obscuration testing, we attempted to coat the RCL-9 hydrophilic TiO₂ particles with DPDMS by dissolving organosilane in SCCO₂, followed by coating and drying with SCCO₂. It is well known that fluorinated surfactants (FS) render otherwise hydrophilic surfaces extremely hydrophobic. Heptadecafluoro-1,1,2,2-tetrahydrodecyl trimethoxysilane, CF₃(CF₂)₇-CH₂CH₂-Si-3(O-CH₃), was selected as the fluorinated molecule for coating the RCL-9 TiO₂ from SCCO₂.

A literature review was conducted on the coating of TiO₂ particles with organosilanes from SCCO₂. The method disclosed by Domingo et al. (2006) was used for the surface treatment of TiO₂ particles. The procedure involves first coating the particles with the organosilane followed by drying in SCCO₂. The major variable investigated was the coating or exposure time to DPDMS. Subsequently, the samples were characterized for moisture content and settling time and the endpoint was measured by the Tyndall effect. Table 18 shows the results from the coatings studied.

Table 18. Coating RCL-9 DPDMS

Number	Silane Contact Time (min)	Drying Time (min)	Moisture (%)	Settling Time (s)
BAC - 9650 - 2010 - 1	15	0	0.428	1173
		30	0.212	3208
BAC - 9650 - 2010 - 2	50	0	0.322	2181
		30	0.199	4094
BAC - 9650 - 2010 - 3	120	0	0.288	2566
		30	0.111	3579
BAC - 9650 - 2010 - 4	240	0	0.231	2259
		30	0.076	3503
RCL-9/DPDMS as is (Army)		0	0.428	1405
RCL-9/DPDMS (Army); SCCO ₂ dried		30	0.086	3030

Evaluation of the data in Table 18 showed that:

1. As the silane reaction time increased, the residual moisture content in the treated TiO_2 particles was reduced. This was not surprising if it was assumed that there was increased hydrolysis with surface-adsorbed water and increased reaction time.
2. The moisture content was also reduced further after the drying step with SCCO_2 .
3. The settling time for TiO_2 coated with DPDMS from SCCO_2 was greater than for as-received RCL-9 coated with DPDMS by the Army.
4. Settling times for dried $\text{TiO}_2/\text{SCCO}_2/\text{DPDMS}$ were the longest measured in the laboratory, which suggested an increased yield in small particles when using this coating technique. Performance in the Army laboratory will be the key measure of success for this approach.
5. Overall, the settling time for coating DPDMS vs moisture content behavior was similar to the drying of precoated TiO_2 particles (Figure 12). In other words, keeping the moisture level below about 0.25% will decrease agglomeration and increase the yield of small particles.

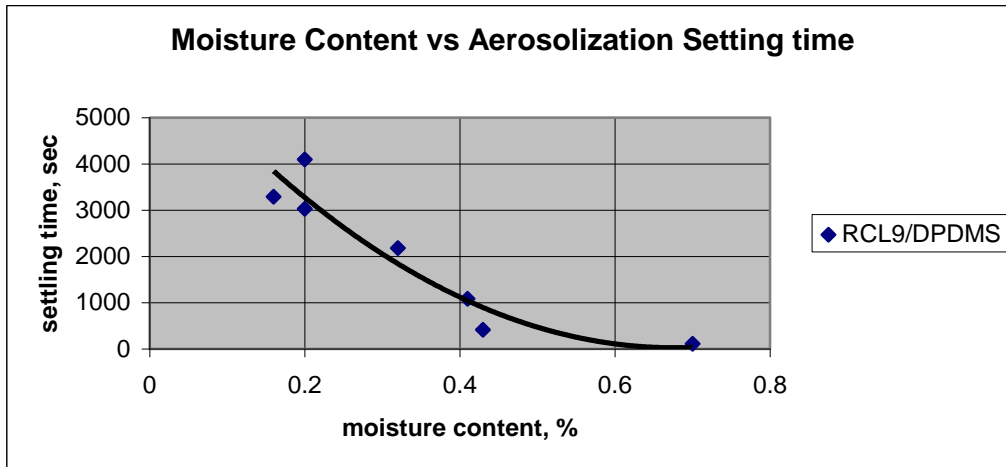


Figure 12. Settling time vs moisture content for coating DPDMS from SCCO_2 .

5.2 Coating and Drying of Particles in SCCO_2 with Agitation

A 500 mL reactor system was modified to allow the coating of silanes accompanied by agitation with a flat blade impeller. The impeller was moved up and down in the vessel and was located at one-third the distance from the bottom of the vessel. RCL-9 TiO_2 particles were coated with DPDMS and FS. The coated particles were characterized by (a)

moisture content, (b) settling time (laser endpoint), and (c) settling characteristics of bulk of the particles over 2 min.

The data for coating DPDMS and FS, with and without agitation in the reactor, are shown in Table 19. Evaluation of the data showed:

1. Coating DPDMS with and without agitation did not appear to change the short- and long-settling behavior.
2. Coating with this fluorosilane did not yield the long- and short-settling time behavior observed with DPDMS coating. The data are suggestive of a more agglomerated particle mix with FS-coated particles vs DPDMS-coated particles.

Table 19. Coating RCL-9 with DPDMS and FS from SCCO₂ with and without Agitation

Material	Moisture (%)	Recovery in 30 s (%)	31–60 s (%)	61–90 s (%)	91–120 s (%)	Settling Time (min)*
RCL-9/DPDMS (as received)	0.323	74.1	14.8	9.3	1.9	32.93
SCCO ₂ Dried DPDMS	0.108	56.1	19.7	16.7	7.6	61.47
RCL-9/DPDMS from SCCO ₂ ; no stir (a)	0.218	40.6	21.9	17.2	20.3	63.13
RCL-9/DPDMS from SCCO ₂ ; no stir (b)	0.248	13.9	11.1	41.7	33.3	67.82
RCL-9/DPDMS from SCCO ₂ ; stir	0.165	52.2	14.9	17.9	14.9	68.83
RCL-9/FS; no stir	0.252	80.5	12.2	7.3	0.0	38.12
RCL-9/FS; stir	0.221	52.4	19.0	11.9	16.7	48.38

* Settling time determined as the end of Tyndall effect when using laser light

6. ECBC TESTING OF TiO₂ POWDERS IN 190 m³ TEST CHAMBER

As described in the earlier sections of this report, 1 g samples of TiO₂ particles were initially dried using SCCO₂. The particles were tested for moisture content and aerosolization in the 5 in. diameter cylindrical vessel, which was designed to evaluate dispersion quality of particles. The settling time for powders was measured as described earlier in this report. It was noted that the settling time increased from a few minutes for as-is particles to >1 h after SCCO₂ drying. The settling time was used as a measure of improved particle dispersion and aerosolization. Scale-up of drying was done to increase from 1 g batches of TiO₂ particles to

15 and 50 g batches. The same two criteria were used to qualify the quality of drying for the larger batches.

After moisture and settling time verification testing in the laboratory, larger quantities of the dried powders were sent to be tested by ECBC in the 190 m³ chamber. The particles were disseminated by SRI nozzle and by explosion of grenades filled with TiO₂ particles. Obscuration was measured as MECs in the SRI nozzle test.

The following were provided as project deliverables to the U.S. Army for testing in grenades and using high-pressure nozzle dissemination. All of the following materials, sent to ECBC, were dry-packaged in the low-moisture transmission packaging that had proven capable of extended dryness retention:

1. 100 g of Tiona 188 (SCCO₂ dried)
2. 100 g of RCL-9/DPDMS (supplied by ECBC and SCCO₂ dried)
3. 100 g of CR470 (SCCO₂ dried)
4. 50 g of RCL-9/DPDMS (coated with DPDMS in SCCO₂ and dried with agitation)
5. 50 g of RCL-9/fluorosilane (coated FS from SCCO₂ and dried with agitation)
6. Evonik T805 (hydrophobic fumed silica)

6.1 Dissemination by SRI Nozzle

Figures 13 and 14 show the MECs for various historical materials evaluated by the Army and supercritically dried CR 470, Tiona 188, and RCL-9/DPDMS.

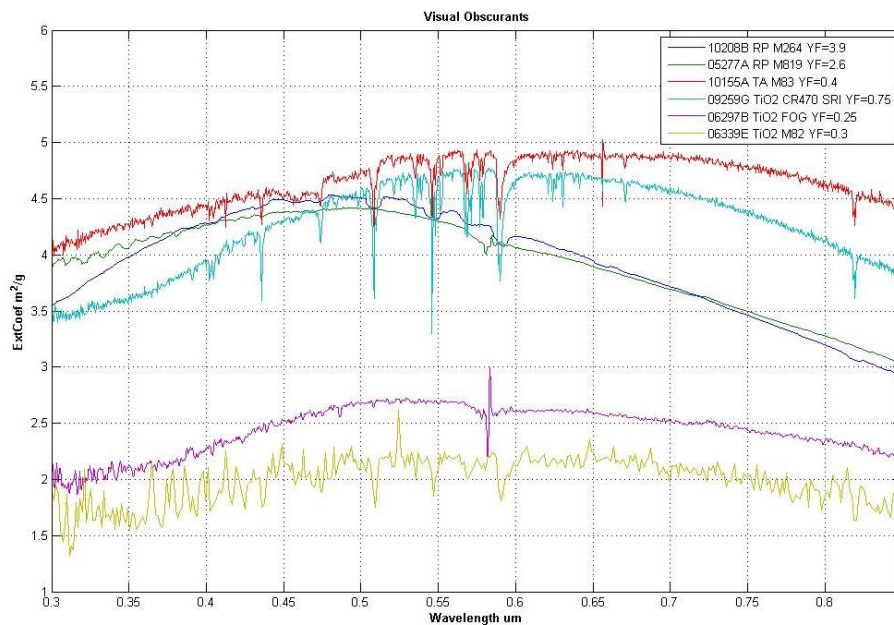


Figure 13. MECs of various TiO_2 particles tested with SRI nozzle in 190 m^3 chamber.

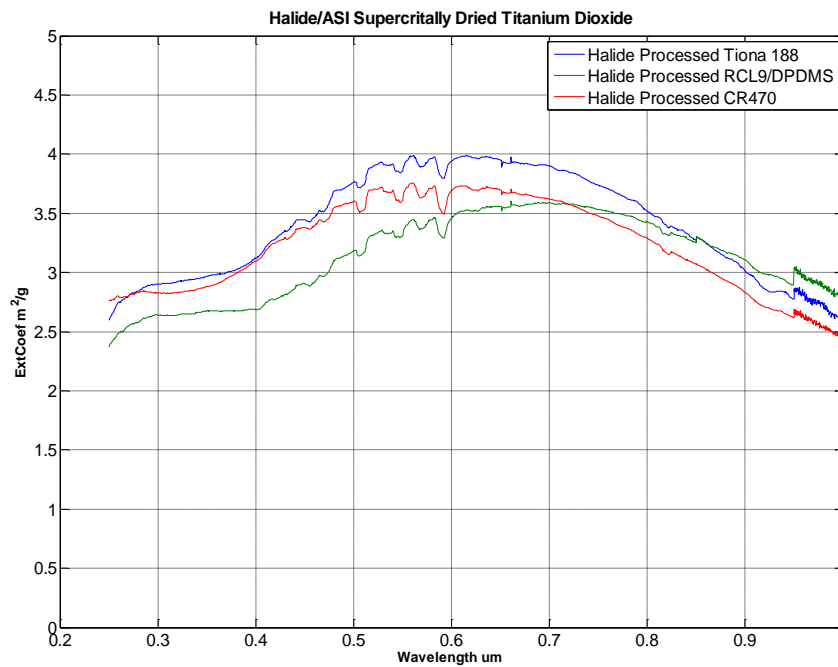


Figure 14. MECs of SCCO_2 -dried TiO_2 particles tested with SRI nozzle in 190 m^3 chamber.

The observations from evaluation of the data in Figures 13 and 14 were:

1. Calculated MEC was comparable for as-is CR470 and SCCO₂-dried CR 470.
2. MECs for the other two materials were comparable to those reported by DeLacy et al. (2011) with the SRI nozzle. Evaluation of Tiona 188 showed the highest MEC with as-is and SCCO₂-dried powders.
3. No improvement in obscuration was observed with SCCO₂-dried TiO₂ particles when compared relative to the “as-is” material.

6.2 Dissemination by Explosives

The particles were also tested in grenades for ED. New grenades with a 50 g capacity were prepared for these tests, and the results are shown in Figure 15. The extinction coefficients for all the SCCO₂-dried materials were low (<1.5). These MECs were lower than those measured by the U.S. Army and are shown in Table 2 as benchmark data. It is not clear if this finding was due to design differences between the 50 and 250 g standard grenades.

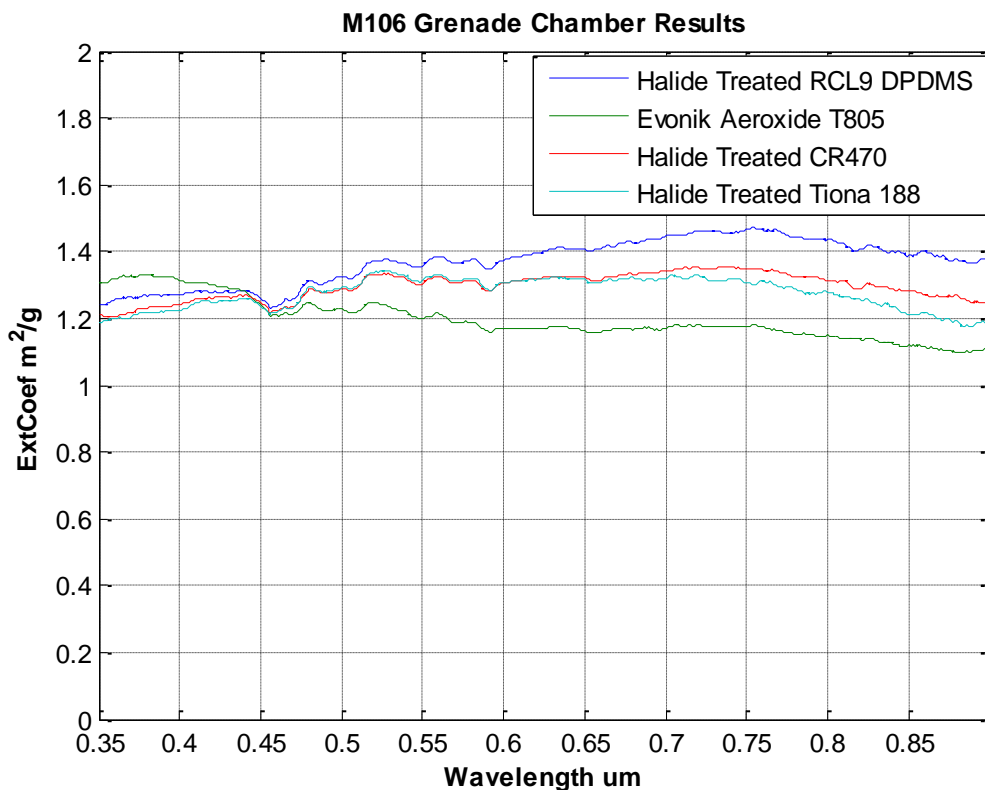


Figure 15. ED tests in 190 m³ chamber.

6.3 Testing Fumed TiO₂

The fumed TiO₂, Evonik T805, was also evaluated by ED with the MEC measured over visible and UV wavelengths and shown in Figure 15. The MEC was extremely low, in the 300 to 500 nm range, which was not consistent with the MECs obtained with the SRI nozzle in the same vessel (MEC ~7.5, Appendix C, Figure C-1). The reasons for this were not clear, but could have been related to the low packing fraction in the grenade with the fumed TiO₂ and the lower refractive index and density. It was also possible that the different design of the 50 g grenade caused this discrepancy.

In summary, SCCO₂ drying was not useful in reducing particle agglomeration and improving the performance of the visual obscuration grenades that were prepared with anatase TiO₂ particles, no matter whether the particles were SCCO₂ dried or coated with silanes from SCCO₂.

7. FUMED TiO₂: SMALLER PARTICLES FOR OBSCURATION

Fumed TiO₂ particles (Evonik P25 and T805; aggregates of ~25 nm particles) and their blends with anatase TiO₂ particles (CR 40 and RCL-9/DPDMS) were dispensed into the Army 190 m³ chamber with an SRI nozzle to evaluate the particles for obscuration effectiveness. The key findings were:

1. The fumed TiO₂ particles had MECs (~7 m²/g) in the 300–500 nm wavelength range.
2. The MECs were reduced to about 4.5 in the visible spectral range (500–700 nm).
3. The particles behaved (scattered light) like 100–200 nm sized particles, which are porous.
4. The blends showed intermediate MECs and should be explored further.

The details of this work are shown in Appendix C.

8. HIGH SHEAR FOR PARTICLE DEAGGLOMERATION

One unanticipated result of the TiO₂ powder characterization work that was performed during this program was to highlight a well-known phenomena—the power of shear forces to disrupt and break apart agglomerated particles.

It was observed that shear forces, sufficient to deagglomerate the test TiO₂ powders to near their fundamental particle size of 0.25 μm, were achieved in the Horiba particle analyzer at gas flow pressures of 40 psig. Testing was performed using higher pressures to see if dispersions of smaller particle sizes could be achieved. The results are detailed in Appendix B.

9. SUMMARY AND CONCLUSIONS

The surface-treated TiO₂ particles selected for investigation in this study were dried by SCCO₂. This drying reduced the adsorbed moisture content of the TiO₂ particles. However, the moisture content of smaller, less agglomerated particles increased slightly after drying with SCCO₂. This was manifested by significant increases in settling times with laser endpoint detection. The re-adsorption of surface moisture onto the test materials was rapid under exposure to ambient conditions, which was particularly true for the hydrophilic TiO₂ materials. This may explain, in part, why the apparent improvement could not be converted into material improvement during the larger scale Army tests in their 190 m³ chamber with aerosolization through an SRI nozzle or via explosive detonation.

Hydrophilic TiO₂ particles were also coated with an organosilane and fluorosilane from SCCO₂. Larger scale testing of these particles did not show superior obscuration performance in tests conducted by the U.S. Army, but did match the performance of the previous Army DPDMS-coated RCL-9 material.

Both the SCCO₂ drying procedure and the process for the silane coating of the hydrophilic RCL-9 TiO₂ were successfully scaled up from 1 to 50 g batch sizes.

We successfully developed a packaging system for dried TiO₂ that does not change the moisture content of the particles over the test period of about 3 months.

We have identified TiO₂ particle deagglomeration by shearing the particles in capillary nozzles at high pressures. This novel route may be useful, not only for deagglomerating particles, but for providing options for disseminating particles from grenades with potentially higher yields of aerosolized particles.

10. IDEAS FOR FUTURE WORK

A fundamental issue is, “Why do the ‘pigment-based’ TiO₂ primary particles that are on the order of 250 nm (0.25 μm) diameter agglomerate into less useful obscurant particles of 0.5 to ≥4 μm, which vary widely in performance; and how can this be undone and/or protected against?” The Horiba particle size results suggest that the use of a 40 psig nozzle produces a much smaller mean particle size (~0.27 μm), with little variation in size distribution.

There are two ideas that should be investigated going forward:

1. Conduct a detailed investigation of the shear-induced “dry” particle deagglomeration of TiO₂ pigment particles and possibly the deaggregation of the larger fumed TiO₂ particles (P25). Both SCCO₂ and dry nitrogen should be used in the evaluation. The use of nitrogen will eliminate the possibility of removing surface treatment molecules from TiO₂ particle surfaces. A new aerosolization system should be installed in the laboratory that can handle the release and recovery of particles from a

high-pressure source and allow for changes in nozzle design. The chamber should incorporate the ability to measure obscuration.

A follow-up to the first idea would be to establish a realistic maximal FoM value for the TiO_2 particles by testing the performance of a “preferred nozzle” on the Army Lab’s 190 m³ chamber.

2. Transfer of the explosive energy from a grenade to the particles and how the powder responds to that transferred energy are significant weak points in the dissemination of TiO_2 particles from grenades. Based on the data shared by the Army, a new way to uniformly couple the energy to the TiO_2 particles is needed so that the yield of TiO_2 particles can be raised. At the time of this study, the maximum yield of particles from ED was close to 20%. At this point, it was not known whether this low value was dominated by an in-canister agglomeration (storage), an impact-driven compressive agglomeration (or aggregation) during detonation, an adiabatic compressive or detonation “thermal effects”, or by a nonuniform (or, conversely, a too uniform) transfer of the detonator energy to the powder mass.

An example of a novel method of particle dissemination would be to incorporate multiple nozzles in a grenade. Pressure could be generated inside the grenade by a chemical reaction (e.g., azide decomposition as in an automotive air bag). Uniform pressure generation inside a chamber may be used to force TiO_2 particles through a series of nozzles, allowing the uniform transfer of energy from the high-pressure gas generated inside the chamber to the TiO_2 particles.

Alternatively, if the hoop stress failure point of the grenade canister is excessive, it may provide an anvil against which the TiO_2 powder is struck by the detonator’s pressure wave, which is suggestive of adding scribed lines to the canister wall to promote controlled failure locations. When combined with “shaped” detonator charges, these early failure zones may be used to serve as nozzles.

Blank

LITERATURE CITED

DeLacy, B.G.; Redding, D.; Matthews, J. *Optical, Physical, and Chemical Properties of Surface Modified Titanium Dioxide Powders*; ECBC-TR-835; U.S. Army Edgewood Chemical Biological Center: Aberdeen Proving Ground, MD, 2011; UNCLASSIFIED Report.

Domingo, C.; Loste, E.; Fraile, J. Grafting of Trialkoxysilane on the Surface of Nanoparticles by Conventional Wet Alcohol and Supercritical Carbon Dioxide Deposition Methods. *J. Supercrit. Fluid.* **2006**, *37*, pp 72–86.

Hobbs, P.; Anand, M. Proposal to SCITECH Services and U.S. Army ECBC for Storage Device Package for Titanium Dioxide (TiO₂) Particles, November 2009.

Blank

ACRONYMS AND ABBREVIATIONS

DPDMS	diphenyldimethoxysilane
ECBC	U.S. Army Edgewood Chemical Biological Center
ED	explosive dissemination
FoM	figure of merit
FS	fluorinated surfactants
HGI	Halide Group, Inc.
MEC	mass extinction coefficient
MVTR	moisture vapor transmission rate
psf	pounds per square foot
RH	relative humidity
rpm	revolutions per minute
SCCO ₂	supercritical carbon dioxide
SEM	scanning electron microscope
SRI	Stanford Research Institute

Blank

APPENDIX A: UNCONFINED YIELD STRENGTH OF POWDERS

Refer to Section 2.3 for a description of unconfined yield strength.

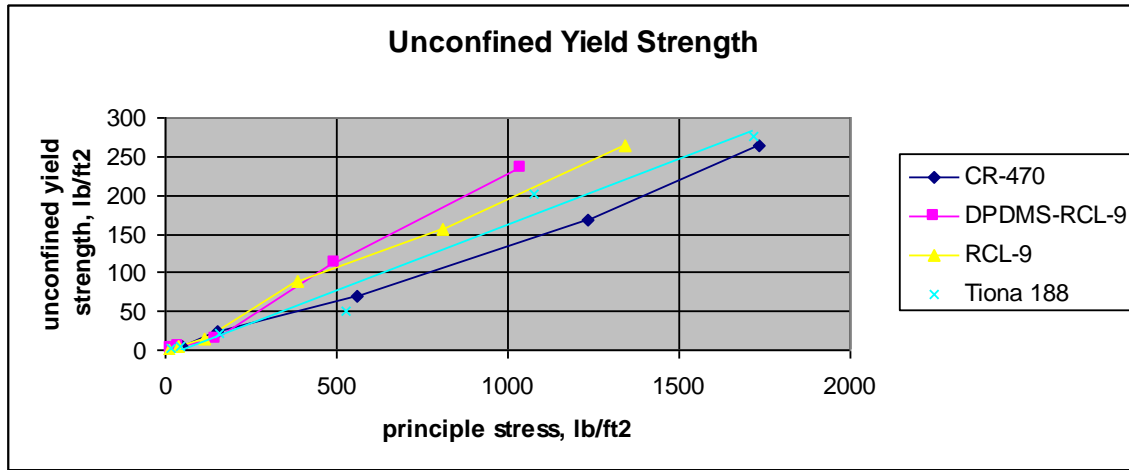


Figure A-1. Calculated yield strength of as-received powders.

For aerosolization of a powder, determination of the magnitude of the interparticle adhesion forces relative to the gravitational forces would be desired. Bulk strength is proportional to the sum of all the particle adhesion and interparticle friction forces per unit volume. The gravitational forces are proportional the sum of all the particle weights per unit volume and should be roughly proportional to the bulk density of the product. The cause of the cohesion (van der Waals, capillary, or fracture) and particle size distribution affect the calculation of these values. Various models describing the particle cohesive forces are shown in Table A-1.

Table A-1. Mechanisms for Particle Agglomeration

Model	Mechanism	Source
$F_c = K_1/D_p^2$	Van Der Waals Forces	Mollerus
$F_c = K_2(C)^{1/2}/D_p$	Capillary forces	Rabinovich
$F_c = K_3/D_p^{1/2}$	Elastic Fracture	Rumpf
$F_c = K_4/D_p^n$	Plastic-Elastic Fracture	Specht

F_c stands for function

K_1 , K_2 , K_3 , and K_4 are proportionality functions

D_p is the diameter of particle

C is the concentration of water or solvent

If the particles that make up the powder to be aerosolized are weakly held together in agglomerates, assemblages of particles can be broken up or separated from each other under the aerosolization forces. In this case, the aerosolization forces will generate multiple smaller particles from the these larger agglomerates. If these smaller particles don't reaggregate, they should more easily remain suspended (aerosolized) or settle more slowly. On the other hand, if the particles are fused or strongly held together in larger masses or

aggregates that can't be disrupted by the aerosolization forces, then the powder should settle more quickly.

When the equations in Table A-1 are considered, the drying of TiO₂ powders should remove or mitigate any capillary forces binding the particles into larger agglomerates. Evaluation of the data in Figure A-2 indicate a decrease in yield strength for all of the tested particles after drying at 110 °C to remove any surface-sorbed moisture. Assuming that this reduction can be attributed solely to a reduction in the capillary forces while none of the other modeled forces of Table A-1 change, an estimate of the contribution of the capillary forces to the overall unconfined yield stress can be made. For the four materials tested in this study, at a principle stress of 1000 psf (pounds per square foot, which is the packing force), the capillary forces contributed ~20% to the unconfined yield stress. (Subsequent testing, which indicated a very rapid surface moisture uptake, particularly on untreated TiO₂ surfaces, suggested that this 20% represents a minimum percentage level contribution.)

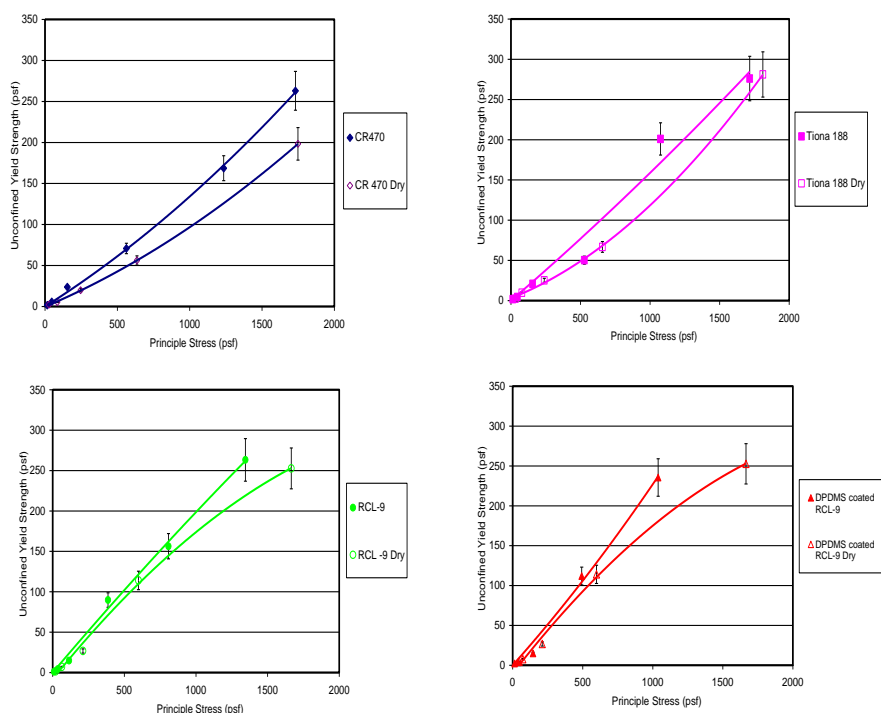


Figure A-2. Drying at 110 °C in an oven decreases unconfined yield strength.

Dividing the yield strength by the bulk density, gravitational constant, and some characteristic length leads to a nondimensional unconfined yield strength value that should scale roughly with the tendency to break up aerosols. Agglomerates in the bulk and wide particle size distributions complicate the analysis, which is where the analysis would become a research project in its own right. This nondimensional unconfined yield strength was calculated using the particle sizes measured in the Horiba dry powder tester. The bulk densities were used as obtained from the unconfined yield strength tester. The results for these are shown in Figures A-3 and A-4.

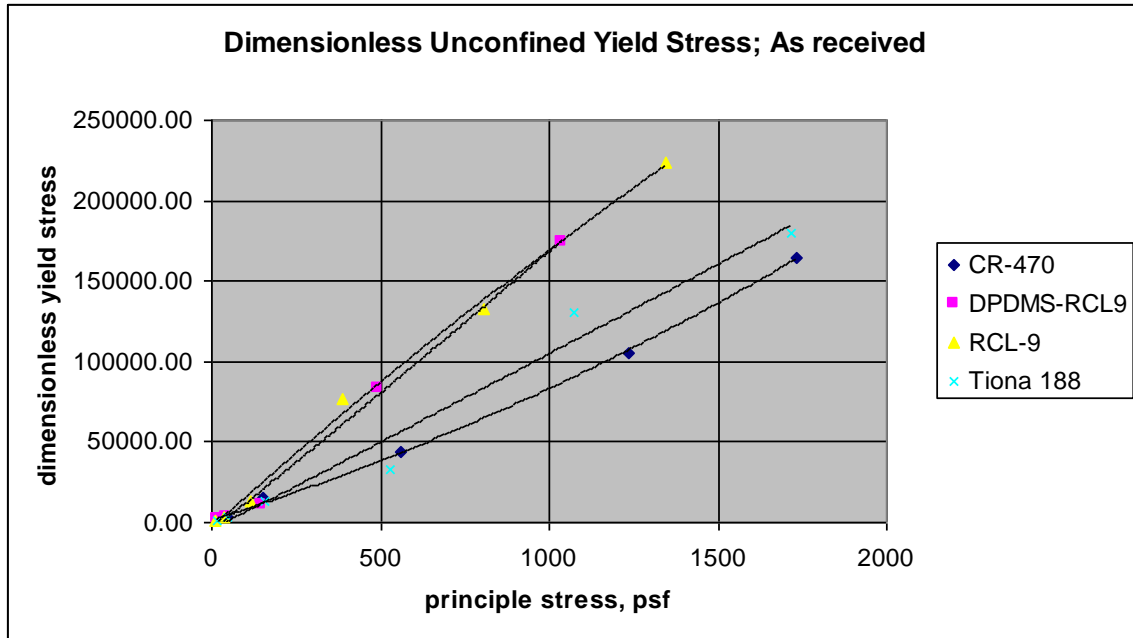


Figure A-3. Dimensionless yield strength.

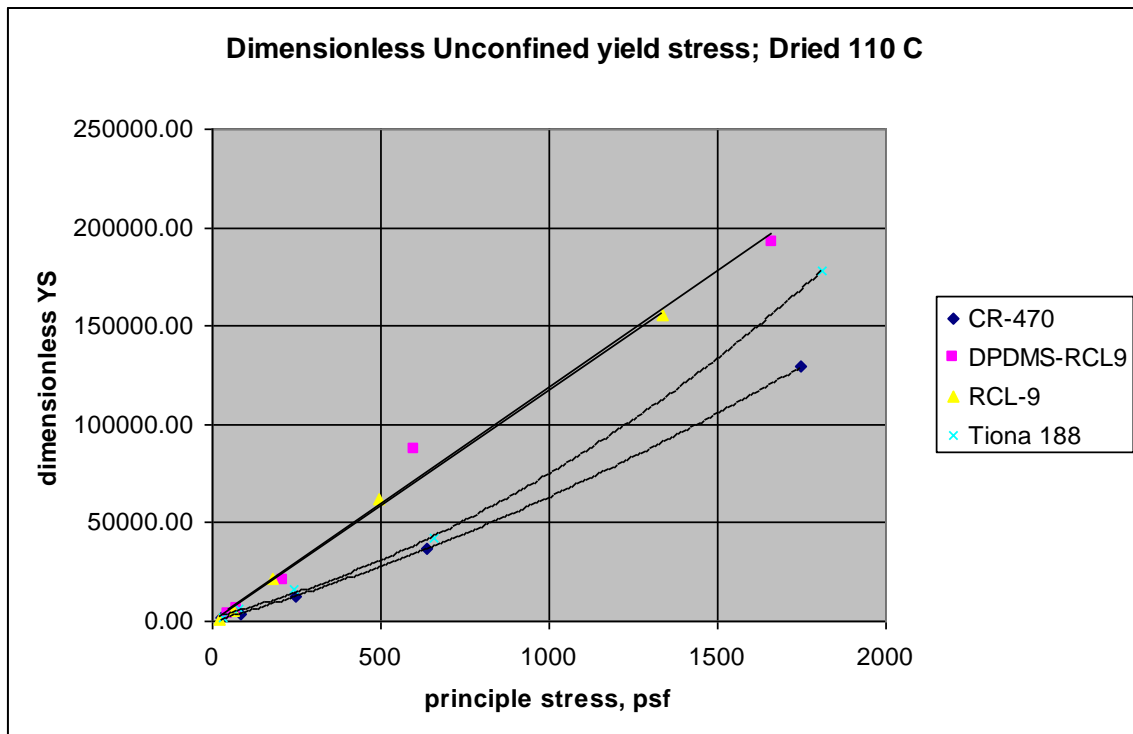


Figure A-4. Dimensionless yield stress for dried powders.

Evaluation of the data again showed that there were differences between the particles, with the lowest yield strength demonstrated by CR-470. After drying, there was a

decrease in yield strength for all of the powders (vs nondried materials). Thus, it appears that there was value in drying the materials prior to use.

We also compared the data generated by DeLacy et al. (2011) on the particle cohesive properties with unconfined yield stress. Table A-2 provides a comparison of data from the DeLacy report with the calculated unconfined yield stress. The most striking observations were: (a) the particle yield stress was lowest for CR 470, which was consistent with the aerosolization results from our laboratory, and (b) the particle yield stress decreased on drying the particles at 110 °C for all four materials tested. Analysis of the data did not show a correlation between the unconfined yield stress and the DeLacy observations related to the cohesive forces on the particles.

Table A-2. Comparison of Unconfined Yield Stress with Particle Cohesive Properties

	Aerated Bulk Density (DV)	Bulk Density (min)	Angle of Repose (DV)	Cohesion (%) (DV)	Flow Index (DV)	Total Flood Index (DV)	As is Unconfined Yield Strength (psf)	110 °C Dried Unconfined Yield Strength (psf)	As-is Dimensionless Unconfined Yield Strength	110 °C Dried Dimensionless Unconfined Yield Strength
RCL-9 (DPDMS)	0.667	0.79	45.5	95.4	26.5	61.5	109.75	78.19	21102	15447
CR 470	0.911	0.88	46.1	88.4	28	56	70.50	50.78	12208	9185
Tiona 188	0.859	0.83	43.5	95.5	44	37	77.27	67.07	14126	11940
RCL-9	0.664	0.62	44.2	68.6	36	51	98.14	71.74	24107	17038

Overall, this device provided limited insight into the properties controlling the aerosolization behavior of the TiO₂ particles; therefore, the effort was abandoned.

APPENDIX B: HIGH SHEAR FOR PARTICLE DEAGGLOMERATION

The concept of applying shear to TiO_2 particles to cause deagglomeration of the particles evolved from several observations in this project:

1. Analysis of TiO_2 particles in the Horiba laser light-scattering apparatus showed essentially the same size and size distribution for all four base materials listed in Table B-1. The particles were introduced into the analyzer via a nozzle at a differential pressure of about 40 psi.
2. The yield of smaller particles increased in the aerosolization chamber as the pressure drop across the particle dissemination nozzle increased. This was manifested by an increase in the settling time of particles. As expected, longer settling times were achieved with smaller particles. In addition, the fraction of particles settling at longer times also increased with the increase in pressure across the nozzle.
3. The yield of small particles by ED from a grenade was much lower than through the SRI nozzle as measured by the U.S. Army in the 190 m^3 obscuration measurement chamber. This was most likely related to nonuniform energy coupling to the particles.

During this project, treatment of TiO_2 particles with SCCO_2 decreased the moisture content of the particles and increased the yield of small particles slightly. This resulted in significantly longer settling times when measured with the laser endpoint detector in the aerosolization chamber. To improve the obscuration performance of the disseminated powders, the yield of smaller particles needed to be increased substantially more than was achieved in this study. Using shear forces to break apart the particles seemed to be a practical route, especially since this concept could be potentially incorporated into the design of the grenade.

A significant body of technical literature describes the use of shear forces and cavitation both to deagglomerate particles and to deaggregate fused particle masses. Although the literature has reported studies of both liquid and gaseous fluid media for providing the shear, commercial systems appear to focus on liquid systems (water) where the shear forces can be maximized. Such equipment is available (e.g., from Microfluidics Corporation, Newton, MA) and achieves particle size reduction by deagglomeration of particles and by the breakup of particle aggregates. Given the focus on minimizing capillary forces between the particles to avoid agglomeration, a “dry” fluid system, such as a supercritical deagglomeration discharge, would be preferred.

A high-pressure nozzle (1/16 in. diameter and 1 in. length) was connected to a source of high-pressure CO_2 in a 24 mL vessel. The TiO_2 particles were mixed with the CO_2 at varying pressures in the vessel (1000 to 5000 psig). Because the vessel was not heated, at these pressures, the CO_2 was in a liquid state. The gas and the particles were released from the vessel into two media: (a) air in the aerosolization chamber and (b) water in a beaker.

Particle Discharge in Air

Discharging particles through the high-pressure nozzle into a vessel could not be done with the current upward “puff” discharge aerosolization chamber because of design limitations. These limitations included the handling of high subcritical to supercritical CO₂ pressures, temperatures $\geq 31^{\circ}\text{C}$, and the height attained by the “puff” on discharge. With pressures of < 50 psig, the puff could reach the top of the chamber, and some portion of the test material would be lodged (lost) in the discharge filter. The aerosolization chamber would need to be redesigned to conduct tests at the high nozzle pressures reproducibly.

A (simple) modified particle dissemination procedure was developed to discharge the TiO₂ particles in a liquid or high-pressure gaseous CO₂ vessel in a downward direction, just above the top of the aerosolization chamber. The TiO₂ powder was driven ballistically while being aerosolized into fine particles, which were then allowed to settle within the chamber. The particles were very fine and mostly deposited on the walls of the chamber, presumably because of static charge. The diameter of the chamber was increased from 5 to 12 in., but much of the powder still deposited on the walls. An insufficient mass of particles was collected from the 1 in. diameter sampling surface at the bottom of the chamber to enable the determination of meaningful particle settling rates.

Thus, some TiO₂ particles were collected on the sticky side of adhesive tape as they were settling in the aerosolization chamber. The sample collection was performed in the early stages of the aerosolization so that the focus would be on the larger aerosolized particles. The particles were analyzed by the Army using a scanning electron microscope (SEM) to obtain some insight into how the particle agglomeration changed after exposure to shear.

Table B-1 shows the pressure and sample conditions at which the particles were sheared through the nozzle. The objective of the work was to determine the effects of pressure drop and sample size. These initial experiments were for screening purposes only so that more detailed work could be done, if the results were encouraging. SEM analysis done by the U.S. Army was inconclusive and could not provide any particle size information or knowledge on how shear helped reduced the particle size after high shear stresses were imposed on the TiO₂ particles.

As a consequence, we decided to discharge particles into water and measure the effect of shear in the nozzle on the particle size.

Table B-1. Shear Conditions for TiO₂ Samples in Air

Sample Number	Material	Amount of Material (g)	CO ₂ Pressure in Vessel (psig)
1	RCL-9/DPDMS (as received)	0.1061	5050
2	RCL-9/DPDMS (SCCO ₂ dried)	0.1018	5070
3	RCL-9/DPDMS (coated and dried with SCCO ₂)	0.0990	5090
4	Fluorosilane-Coated RCL-9	0.0982	5100
5	Tiona 188	0.1100	5080
6	Tiona 188	0.2022	5100
7	Tiona 188	0.4154	5150
8	Tiona 188	0.0991	3110
9	Tiona 188	0.0980	2080
10	Tiona 188	0.1098	1020

Particles Discharged in Water

TiO₂ particles from the high-pressure vessel were also discharged into water. RCL-9 was selected as one of the materials because it is hydrophilic and will allow dispersion of particles. Because of the potential for a significant time lapse between sample preparation and particle size analysis, a surfactant (Tween 80) was added to the water in an effort to reduce particle reagglomeration. No work was done to optimize the amount of surfactant. The second material selected was Tiona 188, a hydrophobic material that did not seem to work very well in obscuration, which indicated that the particles agglomerated.

The particles dispersed in water were analyzed with a Zetasizer (Malvern Instruments Ltd., Worcestershire, UK) by the Army. Just prior to analysis, the particle suspensions were sonicated for 5 min. The suspensions were more than 2 months old before this analysis was done.

In some of the early experiments, Tiona 188 samples were forced through the capillary nozzle at high pressure and formed a stable suspension of the TiO₂ particles in water. This was surprising because Tiona 188 was coated with a surface-active agent that makes the TiO₂ particles hydrophobic. There may have been several reasons for this unusual behavior: (a) If some of the surface active agent was removed from the particle surface by exposure to SCCO₂, this could have exposed hydrophilic TiO₂, which would be capable of dispersing in water. (b) It was also possible that shearing created new particle surfaces that were not coated with the surface-active agent and hence were naturally hydrophilic, allowing dispersion of the sheared TiO₂ particles in water. It would be difficult to determine these effects without more detailed

testing. If some surface-treatment agent was removed by exposure to high-pressure CO₂, more of the surface treatment may be removed at higher CO₂ pressures (greater solubility at higher pressures). Higher CO₂ pressures would result in higher shear forces, presumably leading to greater agglomerate disruption. Table B-2 provides the deagglomeration conditions and the resulting average particle size obtained from the Zetasizer, measured 2 months after the high-shear deagglomeration.

Table B-2. Shear Conditions for TiO₂ Samples in Water and Average Particle Size in Water

Sample	Data File	Number Average Size (nm)
0.1 g RCL-9 w/surfactant – 5000 psi	Halide Sample 1	623.3
0.2 g RCL-9 w/ surfactant – 5000 psi	Halide Sample 2	485.1
0.3 g RCL-9 w/ surfactant – 5000 psi	Halide Sample 3	708.3
0.1 g Tiona 188 – 5000 psi	Halide Sample 4	605.8
0.1 g Tiona 188 – 4000 psi	Halide Sample 6	501.7
0.1 g Tiona 188 – 3000 psi	Halide Sample 5	482.7
0.1 g Tiona 188 – 1000 psi	Halide Sample 7	453.4
0.2 g Tiona 188 – 5000 psi	Halide Sample 8	692.6
0.4 g Tiona 188 – 5000 psi	Halide Sample 9	753.8
0.6 g Tiona 188 – 5000 psi	Halide Sample 10	664.2

Several important observations can be made from the data with Tiona 188 in

Table B-2:

1. The measured particle sizes (450 to 750 nm) were close in size to the individual TiO₂ particles at 250 nm. The particles were far smaller than the size that should be calculated on the basis of either the observed settling time or from the settling rate calculations in the 190 m³ test chamber. The measured particles were also close to the D90 particle size for these materials as measured by the Horiba particle size analysis in Section 2.4 of this report. This result demonstrates the benefit of deagglomeration in a shear field. Additional work is necessary to fully quantitate the degree of deagglomeration. However, the fact that Tiona 188, with its surface-modifying hydrophobic treatment, could be dispersed in water after shear deagglomeration is important. It implies a partial regeneration of typical TiO₂ hydrophilicity either through particulate fracture generating fresh TiO₂ surfaces or by a significant removal of the bound organic treatment layer. The former explanation appears far more likely based on a simple mechanical force explanation. Sonication alone was believed to be lacking in very high levels of cavitation and, therefore, would not disperse Tiona 188 in water, but this needs to be confirmed.
2. The effect of CO₂ discharge pressure on the particle size obtained in water, also shown in Figure B-1, was greater at lower CO₂ pressures (i.e., deagglomeration was more effective at lower CO₂ pressures).

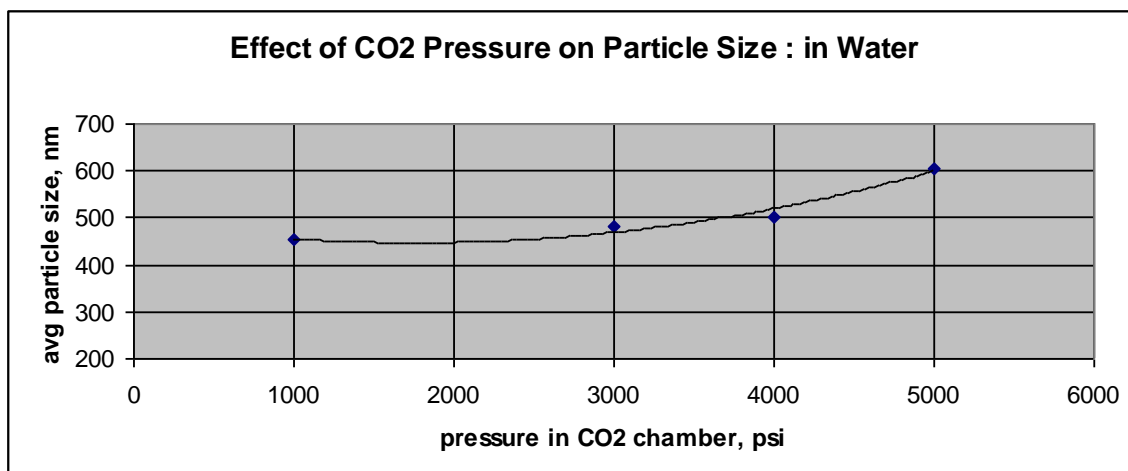


Figure B-1. Particle size of TiO₂ dispersed in water.

The effect of CO₂ pressure was surprising from a mechanical viewpoint. The TiO₂ particle sizes were expected to be smaller as the shear forces increased in the nozzle at higher CO₂ discharge pressures. In the absence of other supporting surface analyses, it was possible to rationalize this data as follows. As the pressure across the nozzle increased, smaller TiO₂ particles were produced and dispersed in water. Aqueous solids dispersions such as these could be notoriously difficult to stabilize, particularly on this time scale. Agglomeration, segregation, and settling can all occur in the absence of optimized surfactant loadings, ionic strength, and pH level. None of these factors were adjusted or optimized for the amount of free surface generated when shearing the particles through the nozzle into the water.

If the analysis using the Zetasizer was performed as soon as the particles were suspended in water, smaller particles would have been possible. However, the gap between sample preparation and analysis was >2 months, which probably allowed reagglomeration of particles in water.

It was also possible that some surface treatment of the TiO₂ particles was removed by exposure to high-pressure CO₂. The solubility or removal of the surface treatment occurs at higher pressures, thereby creating more hydrophilic areas for particle agglomeration.

3. The effect of particle mass processed per batch, at a fixed pressure of 5000 psi, was inconclusive as shown in Figure B-2. However, it was encouraging that the particle size was not affected significantly by the change in batch size from 0.1 to 0.6 g, which suggests that there was sufficient energy in the CO₂ to deagglomerate the particles. This data would help develop an understanding of the amount of energy that would be required for deagglomeration, if the process were to be scaled up.

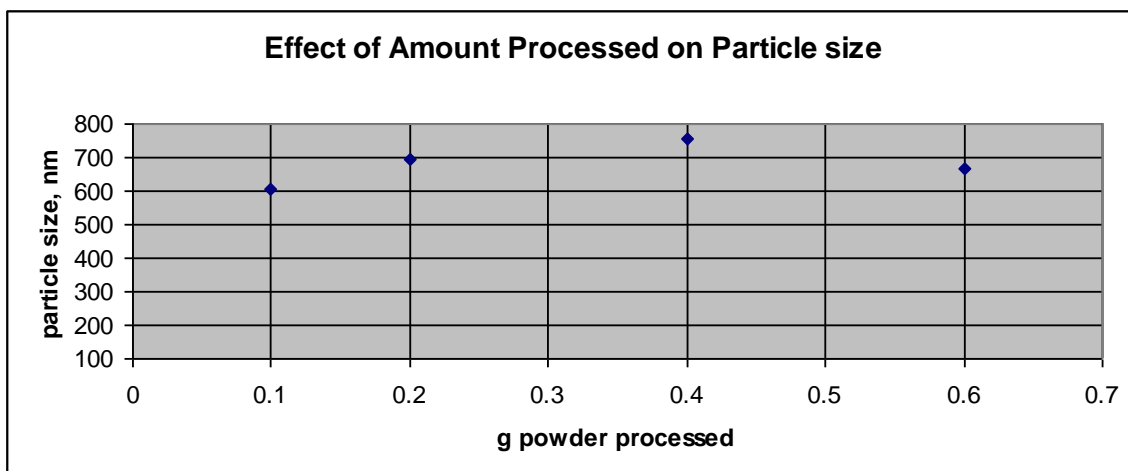


Figure B-2. Effect of batch size on particle size: all at 5000 psi.

4. The data from the hydrophilic RCL-9 particles (with a fixed surfactant load) were not clear; however, it was encouraging to see the particles were small.

More detailed work needs to be done to understand the dynamics of the particle deagglomeration processes, not only in terms of the forces required for the deagglomeration of the desired starting materials, but particularly in terms of designing a scalable process. With sufficient shear, deagglomeration of the larger TiO_2 particle size ($0.25 \mu\text{m}$) and partial deaggregation of a fumed TiO_2 starting material (like P25) would be anticipated. Such a fumed starting material should have light-scattering characteristics because of the primary particle size of $\sim 20 \text{ nm}$ (UV suitable) and the “tunable” reduced aggregate size, such as a size from $100\text{--}250 \text{ nm}$ (visible light suitable). The use of an in-line particle analyzer would be very useful in understanding the value of this potentially new technique for deagglomeration of TiO_2 particles.

APPENDIX C: SMALLER PARTICLES FOR OBSCURATION SUCH AS FUMED TiO_2

The most inexpensive TiO_2 particles available commercially are pigment materials. These are in the more desirable rutile crystalline form and are nominally $0.25\ \mu\text{m}$ in diameter. This is the most desired particle size for visual obscuration (Hobbs, 2009). However, significant agglomeration of TiO_2 powders was observed, such that they behaved like larger particles. Therefore, one objective was to deagglomerate commercial TiO_2 particles by drying or by coating with surface active agents (under zero surface tension) to make them hydrophobic.

Instead of deagglomerating particles, smaller particles could be used as a starting point then allow agglomeration to the desired particle size. Two such commercial TiO_2 particles were selected for evaluation of this concept—Evonik P-25 and Evonik T805 (a surface-modified form of P25). Both of these materials are fumed TiO_2 , with primary particle sizes of approximately $25\ \text{nm}$. However, with these fumed TiO_2 materials, the primary particles aggregate into long chains to form larger masses. The two fumed TiO_2 particles had relatively long settling times in the laboratory aerosolization tester.

As-received (i.e., not dried) P25 and T805 fumed TiO_2 particles were tested in the Army $190\ \text{m}^3$ chamber using the SRI nozzle for particle dissemination. The results are shown in Figure C-1.

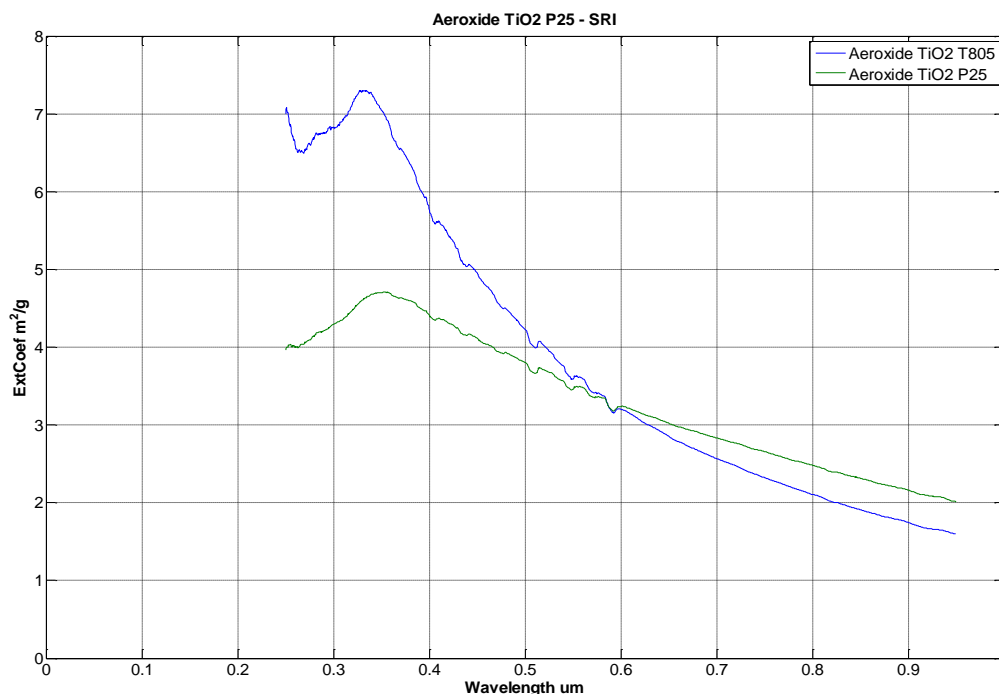


Figure C-1. MECs for fumed TiO_2 .

Evaluation of the data show that the MECs were high ($>7 \text{ m}^2/\text{g}$) in the range of 300–400 nm wavelength (long wave UV). The desired wavelength range for visual obscuration is 500 to 700 nm. In the 500–700 nm wavelength range, MECs were about 3.5 to 4.0 m^2/g . The 7.5 m^2/g MEC for T805 at 350 nm suggested that the particles were “acting” like 120–140 nm particles (based on Mie theory as calculated in DeLacy et al., 2011). Figures C-2, C-3, and C-4 show that the particles were larger, as measured on the Morphologi particle size analyzer (Malvern Instruments Ltd., Worcestershire, UK) and on an SEM (photos courtesy of Brendan DeLacy). This finding was consistent with data reported by Ammar,¹ where the count median diameter of P25 was measured as 1–1.45 μm with a geometric standard deviation of 2.9–3.9. In terms of scattering, the larger particles appeared to behave like porous masses, which was not surprising because fumed TiO_2 particles are aggregates of 25 nm particles with porosity.

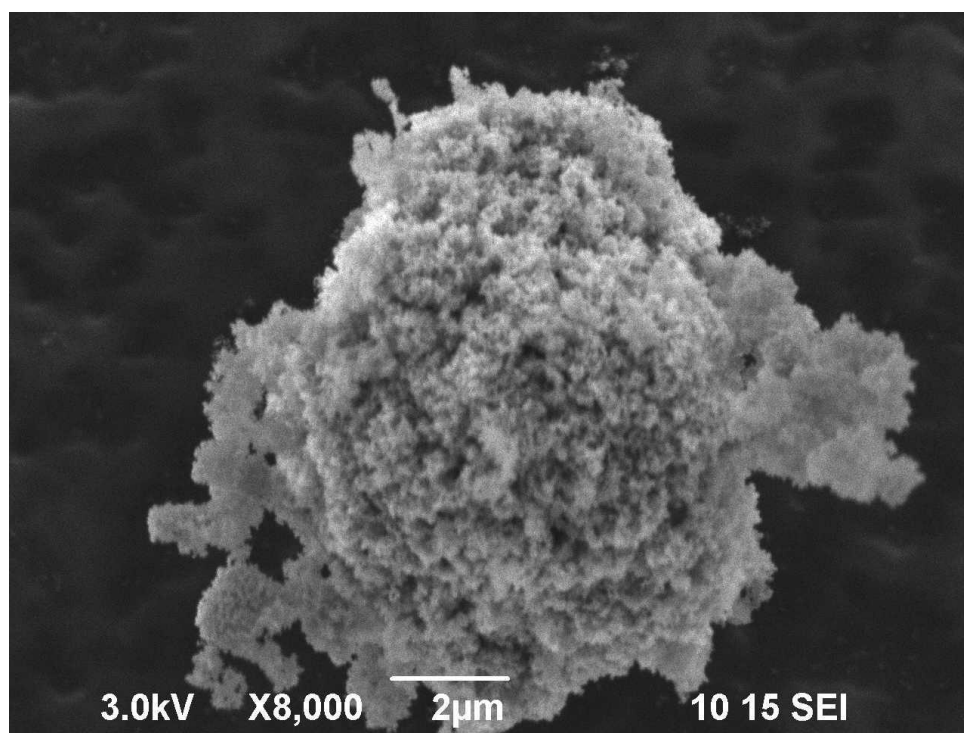


Figure C-2. SEM of T805.

¹ Ammar, Y., et al., *Identification of the Mechanisms for the Breakup of Aerosol Agglomerates in a PWR Steam Generator Tube Rupture*, 6th International Conference on Multiphase Flow, Leipzig, Germany July 9-13, 2007.
http://artist.web.psi.ch/PublicdomainPublications/PSI_Talks_at_Conferences/ICMF/2007/Ammar_2_ICMF.pdf

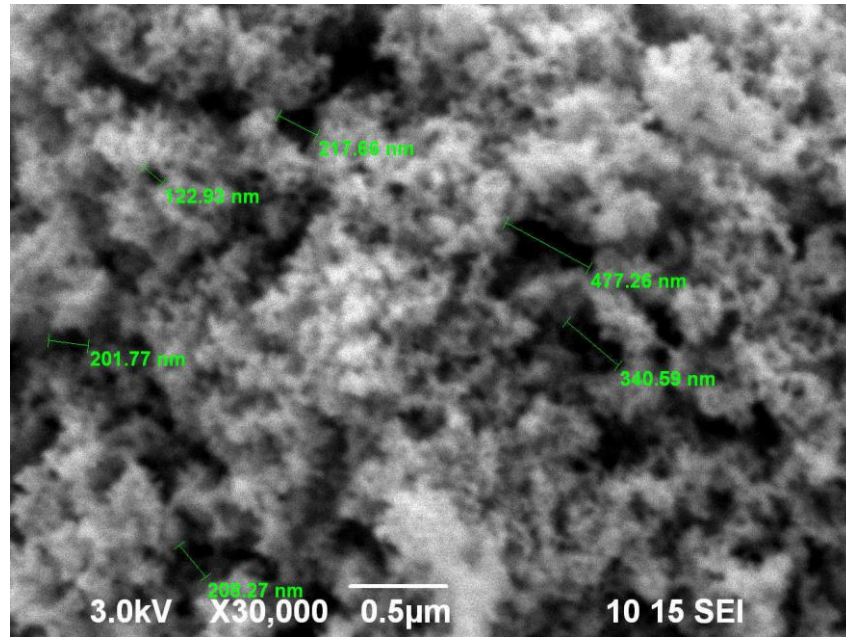


Figure C-3. SEM of T805 showing porosity.

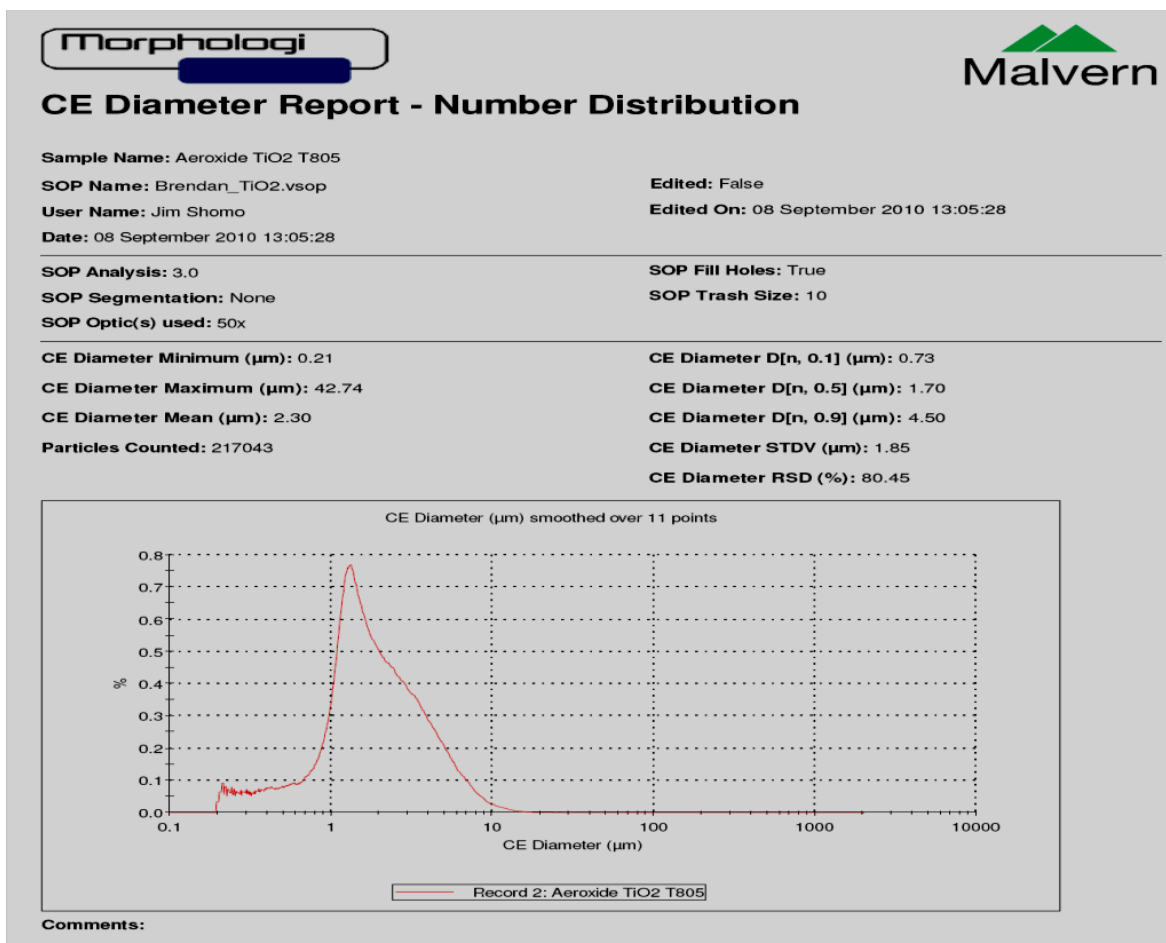


Figure C-4. Particle size analysis.

Blends of T-805 and CR470 and RCL-9/DPDMS were tested with the SRI nozzle to determine whether the mixtures were an improvement in terms of obscuration performance in the visible wavelength range. The results from testing with the SRI nozzle are shown in Figure C-5.

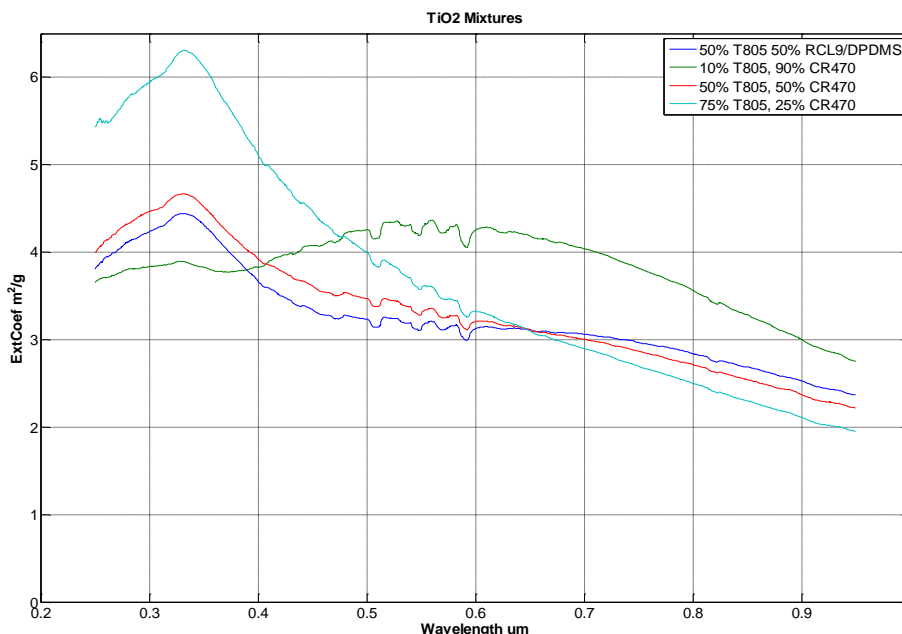


Figure C-5. Blends of fumed and anatase TiO_2 particles.

The best blend had an MEC of $\sim 4.2 \text{ m}^2/\text{g}$ in the range of 500 to 700 nm wavelength, as shown in Figure C-4. This was higher than the extinction coefficient of 3.79 reported by DeLacy et al. (2011) for CR 470. In addition, the extinction coefficient for the RCL-9/DPDMS blend with T805 was lower when compared with the corresponding blend with CR 470. This observation was not consistent with the higher expected extinction coefficient for RCL-9/DPDMS compared with CR 470.

Only a limited amount of exploratory work was done, which should be followed up in more detail because the MECs for some blends were high.

